Clinical Management of Joint Arthroplasty

Veit Krenn · Giorgio Perino

Histological Diagnosis of Implant-Associated Pathologies

EXTRAS ONLINE

Springer

Histological Diagnosis of Implant-Associated Pathologies

Veit Krenn
Giorgio Perino

Histological Diagnosis of Implant-Associated Pathologies

Springer

Prof. Dr. med. Veit Krenn
MVZ für Histologie, Zytologie und Molekulare Diagnostik der überörtlichen BAG für Histologie, Zytologie und Molekulare Diagnostik in Trier, Düren, Düsseldorf
Max-Planck-Str. 5, 54296 Trier, Germany

Giorgio Perino MD
Hospital for Special Surgery
535 East 70th Street, New York, NY 10021, USA

ISBN 978-3-662-54203-3 ISBN 978-3-662-54204-0 (eBook)
DOI 10.1007/978-3-662-54204-0

Springer

Planning: Carola Herzberg
Cover Design: deblik Berlin
Cover Illustration: © Veit Krenn, Trier

Printed on acid-free paper

This Springer imprint is published by Springer Nature
The registered company is Springer-Verlag GmbH Germany
The registered company address is: Heidelberger Platz 3, 14197 Berlin, Germany

Preface

This guide to the histological diagnosis of periprosthetic tissue pathologies in joint arthroplasty is intended to provide a concise, yet comprehensive introduction to the host soft tissue and bone reactions to implants and their wear particulate materials. It is also a practical aid for tissue sampling and processing for the optimal pathological analysis. The target audience comprises orthopedic surgeons, either in practice or in training, as well as clinicians, radiologists, pathologists, and biomechanical engineers who are interested in understanding the details of the histological examination and report.

The text is divided into short chapters providing (a) a broad overview and subtyping of the expanded synovial-like interface membrane (SLIM) proposed as a standardized international classification of pathological changes, (b) criteria for the histological diagnosis of implant infection, (c) response patterns of hypersensitivity/allergic reactions and toxic inflammatory reactions to wear particles and in particular corrosion products, (d) an algorithm for the identification of particles with subclassifications according to their dimensions and morphological features, (e) a practical workflow for the collection and processing of tissue samples, and (f) future perspectives aimed at decreasing the risk of complications and improving outcome with an early and accurate histological diagnosis. Numerous illustrations from our extensive archive of cases are provided for a direct depiction of the criteria used for the identification of both SLIM and particles. Selected references are also provided without the claim of being exhaustive and with the aim of stimulating interest and discussion.

We emphasize the multidisciplinary aspect of the histological diagnosis, which cannot be accurate without the sharing of clinical, laboratory, imaging, and biomechanical data. In fact, this work would not have been possible without the contributions and critiques of all our co-authors and the many colleagues from different medical specialties who have contributed to the development and understanding of this challenging and evolving field of pathology.

We hope that we have succeeded in providing a useful and practical tool for the identification of the many causes of joint implant failures and their revision, and we remain open to any suggestions and criticisms for improvement in the future.

We thank Sylvia Usbeck and Leslie F. Scheuber (Scientific Department and Product Management, CeramTec GmbH) for their constant scientific guidance and valuable suggestions regarding this international multidisciplinary project.

Veit Krenn and Giorgio Perino

Inside:

Histological Diagnosis of Implant-Associated Pathologies

V. Krenn[1], G. Perino[2], P. Thomas[3], M. Thomsen[4], M. Huber[5], T. Gehrke[6], A.Trampuz[7], T. Hügle[8], J.P. Kretzer[9], F. Boettner[10], R.Tikhilov[11], A. Kusaba[12], S. Sesselmann[13]

1 Center for Histology, Cytology and Molecular Diagnostics, Trier, Germany
2 Department of Pathology and Laboratory Medicine, Hospital for Special Surgery, New York, NY, USA
3 Clinic for Dermatology and Allergology, Ludwig-Maximilians-University, Munich, Germany
4 Mittelbaden Clinics Baden-Baden, Trauma and Orthopedic Surgery Units, Germany
5 Institute of Pathology and Bacteriology, Otto Wagner Hospital, Vienna, Austria
6 HELIOS Endo-Clinic, Hamburg, Germany
7 Interdisciplinary Center for Septic Surgery, Charité University Medicine, Berlin, Germany
8 Osteoarthritis Research Center, University Hospital of Basel, Switzerland
9 Laboratory of Biomechanics and Implant Research, University of Heidelberg, Germany
10 Adult Reconstruction and Joint Replacement Division, Hospital for Special Surgery, New York, NY, USA
11 Vreden Russian Scientific Research Institute of Traumatology and Orthopedics, Saint Petersburg, Russia
12 Department of Rheumatology, Zama General Hospital, Japan
13 Department of Orthopedic Surgery, Friedrich-Alexander-University Erlangen-Nuremberg, Germany

Author

Veit Krenn, MD, PhD, Professor of Pathology

Veit Krenn, born in Philadelphia, Pennsylvania, USA, studied human medicine at the University of Vienna (Austria) followed by doctoral studies and teaching qualifications at the University of Würzburg (Germany).

- 2000–2005: Specialist Professor (C3) of Pathology of Infectious Diseases at the Charité Berlin (Charité University Medicine Berlin).
- Since 2005 a member of the executive board of the Center for Histology, Cytology, and Molecular Diagnostics, a health-care center in Trier.
- Founder and speaker of the Orthopaedic Pathology Working Group (German Society of Pathology) and the Rheumatism Pathology Working Group (German Society for Rheumatology).
- Expert pathologist of Working Group 11 (German Society for Orthopedics and Orthopedic Surgery).
- Publisher of a pathology textbook (Pathology of the Locomotor System, De Gruyter), co-author of a histopathological standard reference book (established by Remmele, 3rd ed., Springer), and co-author of four orthopedics/rheumatology reference books: Expertise in Orthopaedic Rheumatology (Springer, 1st ed.), Interdisciplinary Clinical Rheumatology (Zeidler, Zach and Hiepe, 2nd ed.), Guideline for Clinicians: Arthroplasty (Krukemeyer and Möllenhoff), and Metal-on-Metal Bearings (Springer). To date, Prof. Krenn has about 179 publications listed in PubMed.
- Professor Krenn specializes in the histopathology of orthopedic pathology, focusing on the development of diagnostic classification and scoring systems: With his working group and in cooperation with clinical colleagues, he has developed six diagnostic classifications used internationally for chronic inflammatory joint diseases (synovitis score), for arthroplasty pathology (consensus classification of the periprosthetic membrane/synovial fluid), for prosthesis-associated arthrofibrosis, for bacterial low-grade infection (CD15 focus score), and the degeneration score for fibrocartilage as well as the joint particle algorithm.

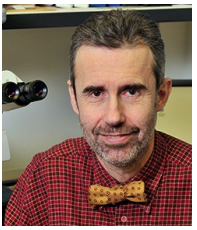

Giorgio Perino, MD, Assistant Professor of Pathology

Giorgio Perino, born in Bologna, Italy, studied human medicine at the University of Bologna. His postgraduate studies in Italy comprised experimental and clinical oncology, the epidemiology of occupational diseases, and anatomic pathology, followed by postgraduate work in anatomic pathology and bone and soft tissue pathology at Mount Sinai Hospital, Hospital for Joint Diseases, and Memorial Sloan Kettering Cancer Center in New York City, NY, USA.

- 2001–2016: Assistant Professor at Hospital for Special Surgery, New York, NY, USA.
- Dr. Perino specializes in the histopathology of experimental and clinical orthopedic pathology, focusing on the histological analysis of experimental animal models for implant infection, intervertebral disc pathology, placental pathology, and osteoarthritis. His clinical research includes the molecular characterization of synovial inflammatory disorders and the elemental analysis of periprosthetic tissue reactions to joint arthroplasty wear material (adverse local tissue reactions and osteolysis) and wear particle biological responses. To date, Dr. Perino has about 40 publications listed in PubMed.

Table of Content

Histological Diagnosis of Implant-Associated Pathologies

Veit Krenn, Giorgio Perino

1 Introduction

Joint replacement is the most successful operation performed worldwide to restore mobility for patients with end-stage osteoarthritis. A sharp increase in the demand for total hip and knee arthroplasty – without including other major joints such as the shoulder, elbow, and ankle – has been projected in the United States between 2005 and 2030, estimated to grow by 137% and 601%, respectively, with the revision rate doubling for both. A similar prediction for revision surgeries has also been made for England and Wales [1], [2]. The economic burden of revision arthroplasty will increase substantially in the near future and pose a real public health problem, which is currently a largely unaddressed issue.

In the Anglo-American literature, synovial tissue, regenerated synovial tissue, and the periprosthetic membrane are referred to using the term "synovial-like interface membrane" (SLIM). Standardized histological examination of the pathological changes of the SLIM is an important tool for determining the causes of implant failure and providing a report useful for implant registries and public health agencies; it also serves as a base for the advanced analysis of implant wear and molecular gene expression and cytokine production [3], [4]. In particular, adverse local tissue reactions (ALTR) to implant materials can be identified and classified histologically by the presence of characteristic patterns and diagnosed using the expanded SLIM consensus classification [5], [3]; implant materials can be classified and quantified with the use of the particle algorithm [6]. The histological diagnosis of morphological changes in periprosthetic tissue and the basic characterization of the wear particles provide a reliable and reproducible set of data useful for (a) determining the causes of implant failure in combination with biomechanical studies, (b) addressing relevant clinical and therapeutic issues, and (c) establishing a common platform for ad hoc analyses in single-center and multicenter studies.

This guide is intended to aid all surgeons who specialize in joint arthroplasty in the interpretation of the report of the histological examination. It also provides a practical tool for the standardized collection and processing of tissue samples to be used for the histological analysis of the periprosthetic tissue.

2 Interdisciplinary Diagnosis of Joint Prosthesis Pathology

2.1 General Principles

The histological examination provides essential information used to clarify the multifaceted pathogenesis of implant failure [7], [8]. This analysis needs to be integrated with clinical, allergological, microbiological, imaging, and biomechanical findings for optimal results. Therefore, the information from the other studies provided by the orthopedic surgeon is crucial for a more accurate interpretation of the pathological analysis. The classification of the histological patterns and the wear particle contents of the periprosthetic tissue can be efficiently and accurately performed using the expanded SLIM consensus classification and the particle algorithm [3], [5], [6].

2.2 International Expanded SLIM Consensus Classification

A broad etiological spectrum of implant-associated pathologies is defined using differential diagnosis criteria based on histological and histochemical criteria (Fig. 1). Histological analysis of the tissue changes and their histological differentiation into wear-induced, infection-associated, immunological adverse reaction (allergic/hypersensitivity and non-allergic), and indifferent type give the surgeon valuable information about the possible causes of the implant/host reactions and also for the patient's clinical management.

The classification of the synovial-like interface membrane (SLIM) allows for the definition of a spectrum of clinically relevant histological diagnoses of implant-associated pathology. The following patterns of periprosthetic tissue reactions are included in the SLIM classification:

- Wear-induced synovitis/SLIM (type I)
- Infection-induced synovitis/SLIM (type II)
- Mixed synovitis/SLIM (type III)
- Indifferent (not wear-induced, not infection-induced) synovitis/SLIM (type IV)
- Prosthesis-associated arthrofibrosis (type V)
- Adverse local tissue reactions to implant wear particles (type VI)
- Local osseous pathologies (type VII)

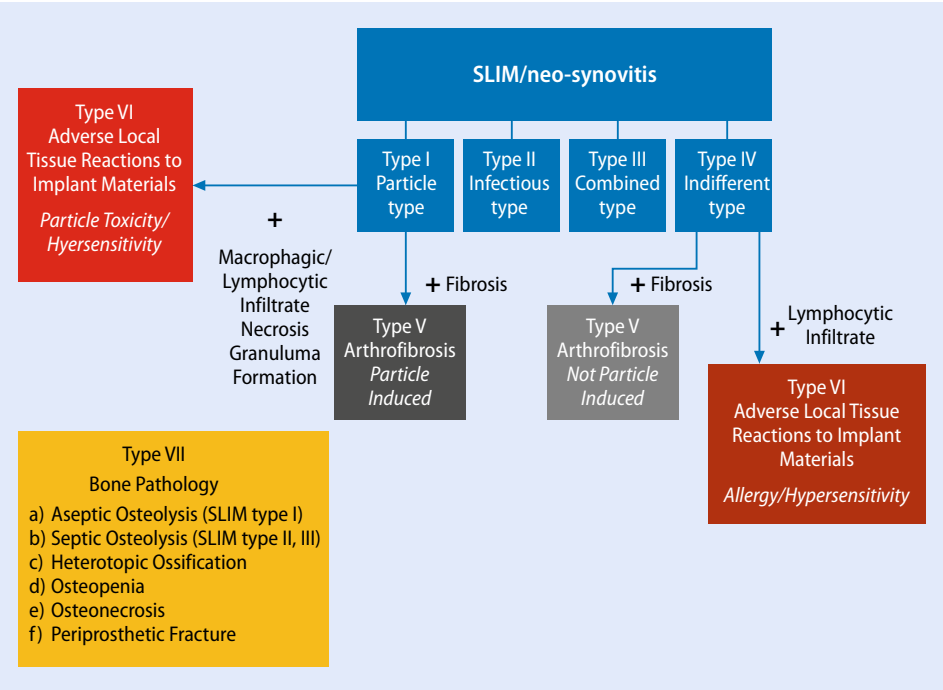

Fig. 1 The international expanded classification of the synovial-like interface membrane (SLIM)

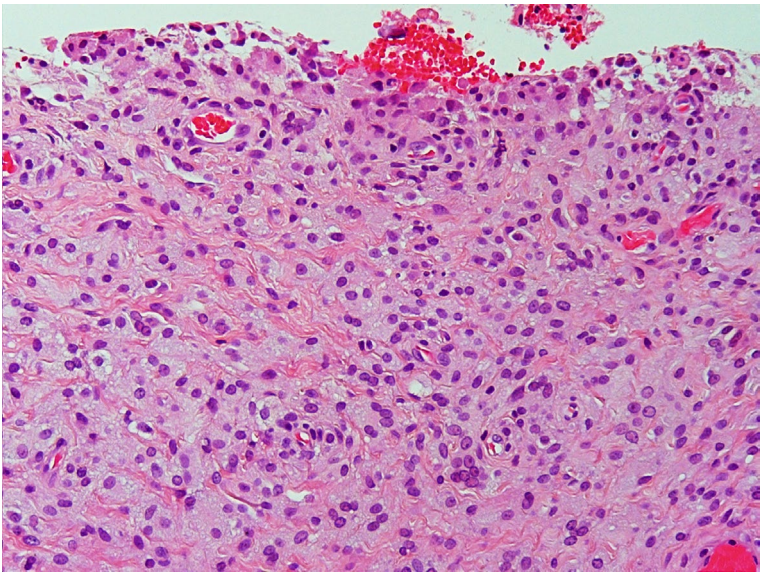

Fig. 2 SLIM type I. Neo-synovial membrane filled with a florid macrophagic infiltrate containing implant wear particulate material (H&E, ×200)

2.3 Wear-Induced Synovitis/SLIM (Type I)

Wear-induced synovitis is characterized by a macrophagic infiltrate with or without multinucleated foreign-body giant cells representing more than 20% of the surface area of the SLIM and often associated with wear-induced implant loosening [3], [5], [6]. Accumulations of wear particles of various sizes can be detected in the cytoplasm of the macrophages and/or giant cells with or without the presence of scattered lymphocytes and/or plasma cells (Fig. 2). The so-called wear-induced necrosis may be present, characterized by a central area of fibrinoid necrosis/infarction lined by palisading fibroblasts and macrophages, similar to rheumatoid nodules. Variable quantities of wear particles can be found in the necrotic areas, most frequently of polyethylene. The differential diagnosis with a mycobacterial or a mycotic infection may need to be considered in the case of wear-induced necrosis with a necrotizing granuloma-like appearance [3].

2.4 Infection-Induced Synovitis/SLIM (Type II)

The histological diagnosis has been considered as a definite diagnostic component of periprosthetic tissue infection [8], [9]. This diagnosis must be seen as complementary to the microbiological diagnosis, and since it is not based on direct detection of pathogens it is less specific, nevertheless facilitating the assessment of the inflammatory infiltrates usually associated with infection. It is also used for frozen section examination in cases when

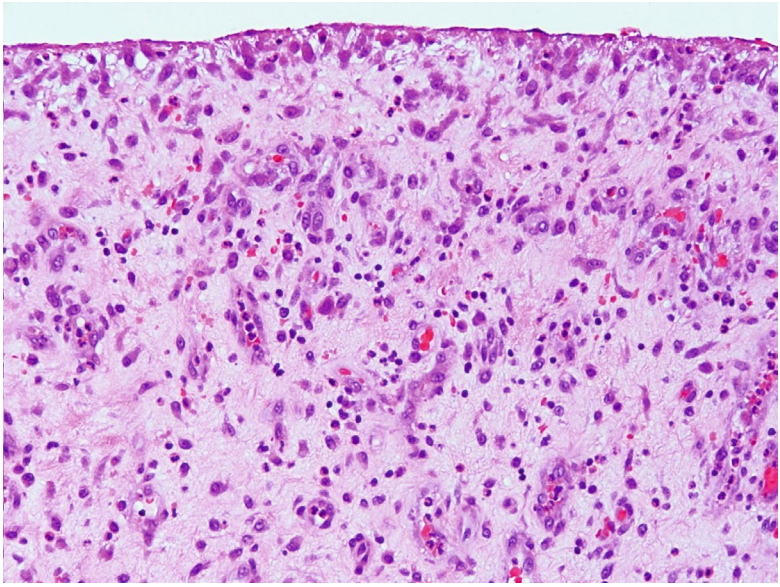

Fig. 3 SLIM type II. Neo-synovial membrane showing loss of lining cell layer, edema, reactive fibrovascular tissue, and polymorphonuclear leukocyte infiltrate (H&E, ×200)

infection is suspected during surgery or for confirmation of its resolution in the two-stage revision procedure. The main focus is on detecting and quantifying the presence of polymorphonuclear leukocytes (PMN). Although direct microbial typing using special enzyme histochemistry staining techniques may be possible in principle, it is generally limited to fungal or mycobacterial infections. Polymerase chain reaction (PCR)-based techniques with sequencing/hybridization of the amplifications enable definitive microbial typing using formalin-fixed and paraffin-embedded (FFPE) tissue samples as well, although the relatively low sensitivity must be taken into account [10].

Low-grade and high-grade purulent, abscess-forming types of inflammation must be differentiated. The former can be difficult to diagnose with accuracy and it is characterized by a predominant chronic inflammatory pattern featuring absence or a slight amount of fibrinous exudate, loss of lining cell layer, edema, formation of granulation tissue with activated fibroblasts, vascular proliferation, and a subtle inflammatory infiltrate of PMN, often associated with plasma cells and small lymphocytic aggregates (Fig. 3). The criteria for the histological diagnosis of infection are detailed in section 2.10.

2.5 Mixed Synovitis/SLIM (Type III)

The histological diagnosis of type III synovitis/SLIM describes a combination of infection and wear-induced synovitis as described for types I and II. A combination of periprosthetic infection and wear-induced reaction is therefore associated with prosthesis failure. The

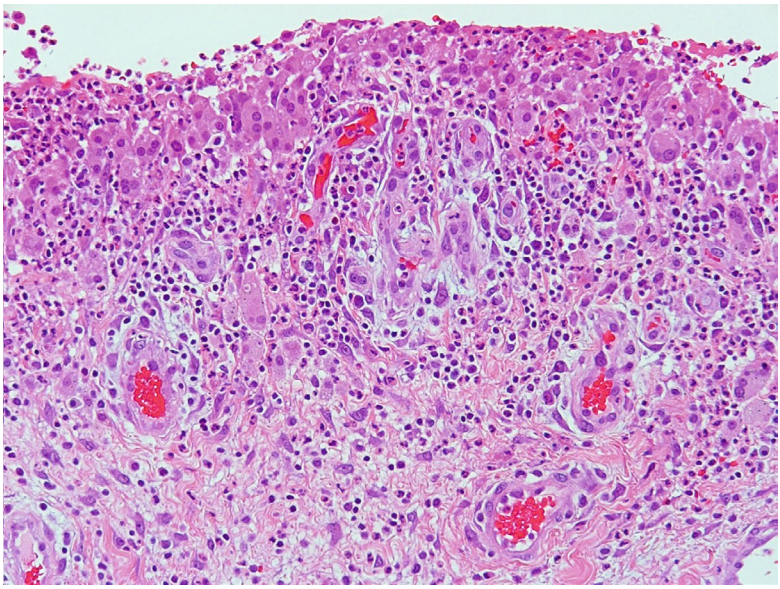

Fig. 4 SLIM type III. Neosynovial membrane with macrophages containing wear particles admixed with PMN inflammatory infiltrate and scattered lymphocytes (H&E, ×200)

diagnosis of infection in these cases is also made using the quantification criteria, particularly for low-grade infections, characterized by a low microbial count and a low PMN count at histological examination. Wear-induced macrophagic infiltrate with or without giant cells and PMN infiltrate are observed histologically in the same areas of the SLIM (Fig. 4).

2.6 Indifferent (Not Wear-Induced, Not Infection-Induced) Synovitis/SLIM (Type IV)

Collagen fiber-rich connective tissue with a low content of bland fibroblasts, in some cases with deposits of hemosiderin pigment (degradation product of red blood cells hemoglobin from hemorrhage), as a substrate of intra-articular bleeding [5] is characteristic of this type of SLIM (Fig. 5). Only occasional PMN, lymphocytes, plasma cells, and macrophages can also be detected without reaching the threshold for the diagnosis of periprosthetic infection. There is no evidence of florid wear-induced reaction. Macrophages and giant cells, when present, occupy less than 20% of the SLIM surface. This pattern is usually observed in cases of complications due to biomechanical or traumatic causes. Prosthesis-associated arthrofibrosis is the most important histological differential diagnosis [3].

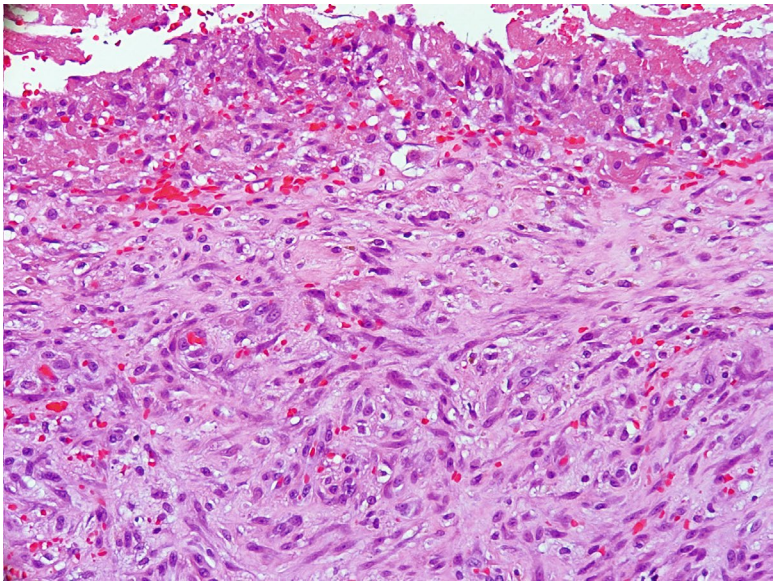

Fig. 5 SLIM type IV. Neo-synovial membrane shows loss of lining cell layer, focal hemorrhage, and florid reactive fibrovascular proliferation (H&E, ×200)

2.7 Prosthesis-Associated Arthrofibrosis (Type V)

Prosthesis-associated arthrofibrosis is clinically associated with a reduced range of motion and/or painful restriction of the range of motion with the knee joint predominantly affected. The prevalence of arthrofibrosis after knee arthroplasty has been reported to be as high as 5–10% [11], [12] and its pathogenesis is still not well understood. Attention is increasingly shifting to the histological, biochemical, and molecular processes underlying arthrofibrosis rather than the previous descriptive model of "adhesions." The cellular and cytokine-based pathogenesis model can offer alternative new therapeutic options in the future, either for prevention or for local control of this complication [13].

Prosthesis-associated arthrofibrosis consists of a pronounced peri-implant or intra-articular fibrous reaction after surgery. The extent of the fibroblastic reaction with ensuing fibrosis of the periprosthetic tissue is variable. The histological diagnosis involves a classification into three grades (mild, moderate, marked) that is based on the density of the fibroblasts (Fig. 6). A correlation between the grading system and the number of β-catenin-positive fibroblasts per high-power field (HPF) at ×400 magnification has been reported with a threshold of ≥ 20 β-catenin-positive fibroblasts per HPF providing a diagnostic sensitivity of 72% and a specificity of 87% [14]. Synovial fibroblasts in arthrofibrosis have also been recently found expressing high fibroblast/myofibroblast transition and xylosyltransferase-I, alpha-SMA protein, collagen type III-alpha-1, and ACTA2 mRNA [13].

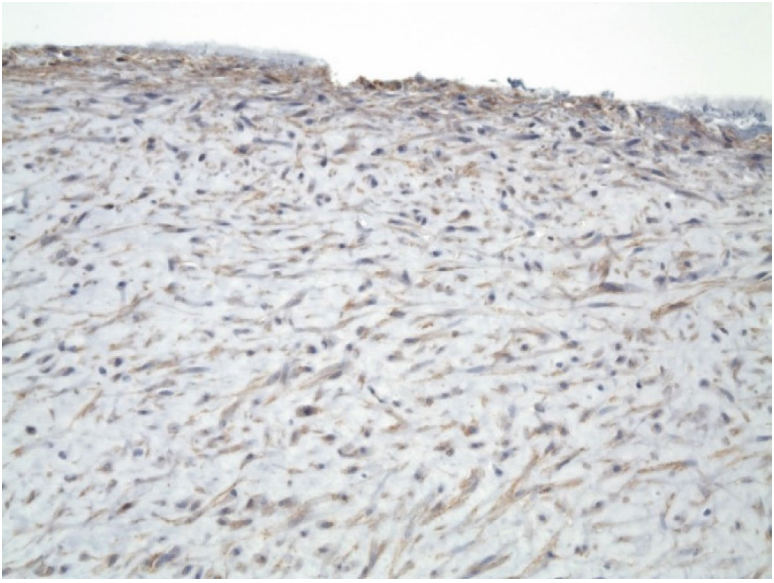

Fig. 6 SLIM type V. Prosthesis-associated arthrofibrosis. Neo-synovial membrane showing high fibroblastic cellularity (grade III) with cytoplasmic expression of β-catenin in a total knee arthroplasty case. The number of cytoplasmic β-catenin-positive fibroblasts by indirect immunoperoxidase reaction is ≥ 20/HPF (×400)

2.8 Adverse Local Tissue Reactions to Implant Materials (Type VI)

ALTRs to implant wear or adverse reactions to metallic debris (ARMD) include a group of inflammatory reactions secondary to wear particle toxicity and/or host immunological hypersensitivity/allergy. They represent an extended classification of the adverse implant reaction originally described as aseptic lymphocyte-dominated vasculitis-associated lesion (ALVAL).

Although the differentiation between particle toxicity and hypersensitivity/allergy would be important, current knowledge of the mechanisms of the reactions and of the physicochemical composition and properties of the particulate material is too limited to allow for a distinct characterization of both, taking also into consideration that some of the reactions might be mixed. Increased metal allergy in patients with failed metal-on-metal (MoM) implants has been reported [15], although metal hypersensitivity testing has been considered not predictive for discriminating between stable and failed total joint replacements [16] and the risk of complications after joint arthroplasty in patients allergic to metals seems to be limited [17]. A consistent association between the presence of corrosion products, defined as tribocorrosion at the MoM-bearing surface and mechanically assisted crevice and fretting corrosion at the trunnion metallic surfaces, the head–neck with or without metallic adapter sleeve (MAS), and metallic cobalt-chromium (CoCr) dual modular neck (DMN) has been reported with differences in the performance of the various implant classes as well as quantitative and qualitative histological differences [4], [18], [19],

[20], [21]. Three histological patterns have been identified: (1) a predominantly macrophagic pattern with absent or minimal lymphocytic response (Fig. 7); (2) a mixed inflammatory pattern, macrophagic and lymphocytic, with variable presence of plasma cells, eosinophils, and mast cells (Fig. 8, Fig. 9); and (3) a granulomatous pattern, predominant or associated with the mixed inflammatory pattern (Fig. 10). In patterns 2 and 3 a population of T cells or of mixed T and B cells has been described with T cells expressing both $CD4^+$ and $CD8^+$ subsets [19], [20], [22], [23]. Of particular interest is the group of cases exhibiting a high number of mast cells and eosinophils with or without formation of perivascular lymphocytic germinal centers, which might represent a reaction to toxic wear with allergic/hypersensitivity components, as recently reported [4].

The histological findings should always be interpreted in the context of all clinical, radiological, microbiological, and allergological data. Valuable data for any class of implants would also be obtained from biomechanical analysis of the corrosion patterns and wear particle characterization by transmission/scanning electron microscopy of the periprosthetic tissue. A multidisciplinary consensus conference with the participation of experts from all specialties involved in the field could also be useful for assessing patient management and treatment, a successful approach already in use for decades for neoplastic diseases.

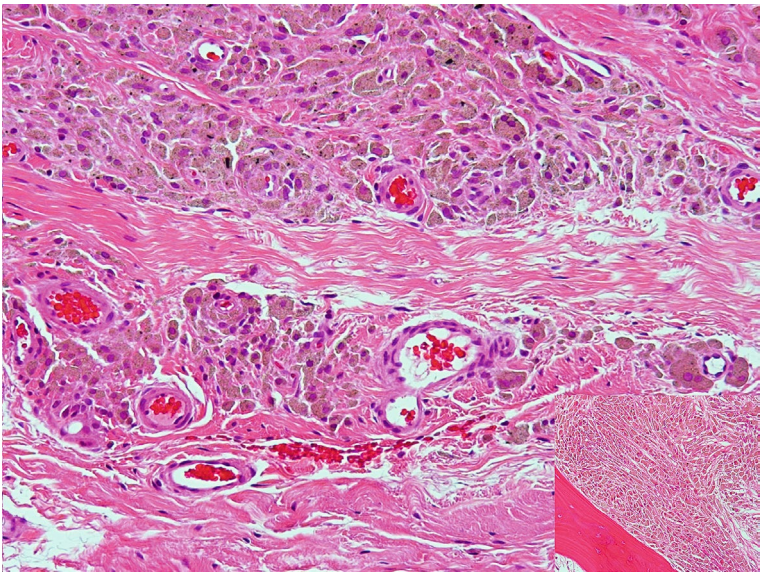

Fig. 7 SLIM type VI. Adverse local tissue reaction: macrophagic pattern with osteolysis. Perivascular macrophagic infiltrate without lymphocytic component (H&E, ×200) and massive osteolysis in *inset* from metal-on-metal implant in hip resurfacing arthroplasty (H&E, ×200)

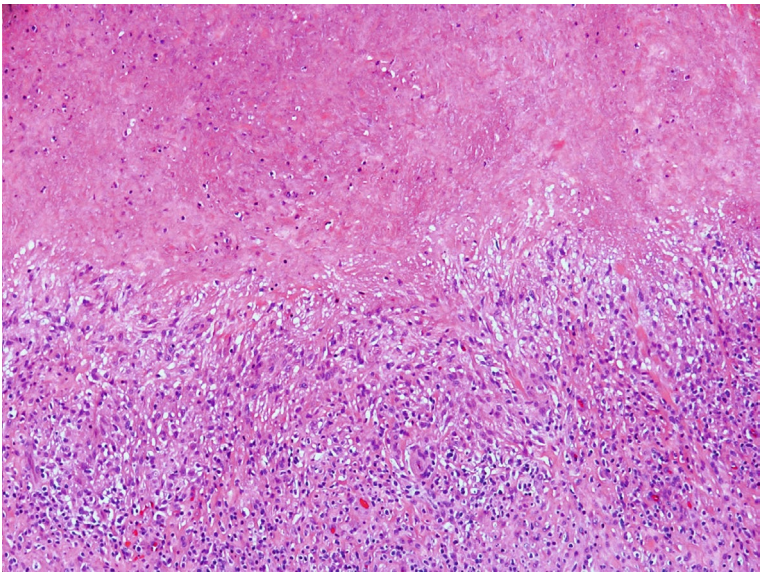

Fig. 8 SLIM type VI. Adverse local tissue reaction: mixed macrophagic/lymphocytic pattern with necrosis. Interface between necrotic zone (*black arrow*) and deep macrophagic and lymphocytic infiltrate from metal-on-polyethylene hip implant with CoCr dual modular neck (H&E, ×100)

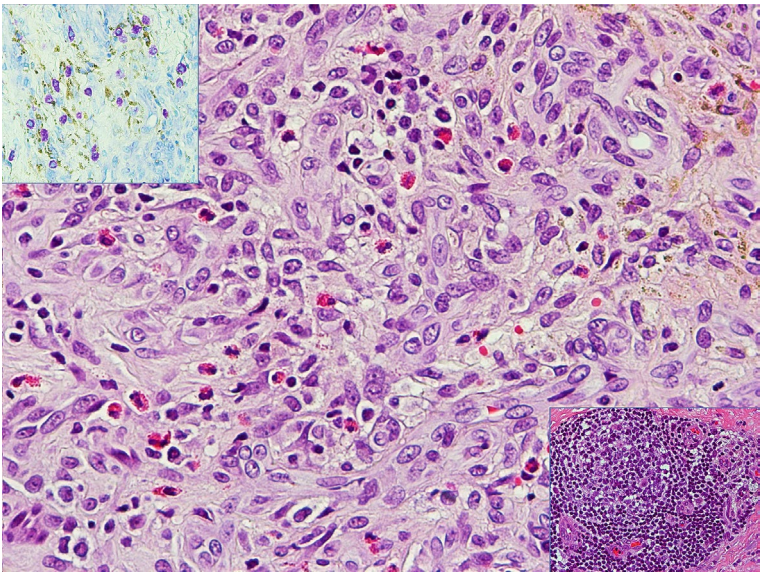

Fig. 9 SLIM type VI. Adverse local tissue reaction: mixed macrophagic/lymphocytic pattern without necrosis and with hypersensitivity/allergy features. Wear particulate debris in a case of a metal-on-metal implant in hip resurfacing arthroplasty implant (time of implantation: 5 months): fibroblasts and macrophages containing globular aggregates of tribocorrosion nanoparticles (*right upper corner*) admixed to numerous eosinophils (H&E, ×200), numerous mast cells in the same area (*left upper corner*; toluidine blue, ×400), and germinal center with tall endothelial cell venules in another area (*right lower corner*; H&E, ×400)

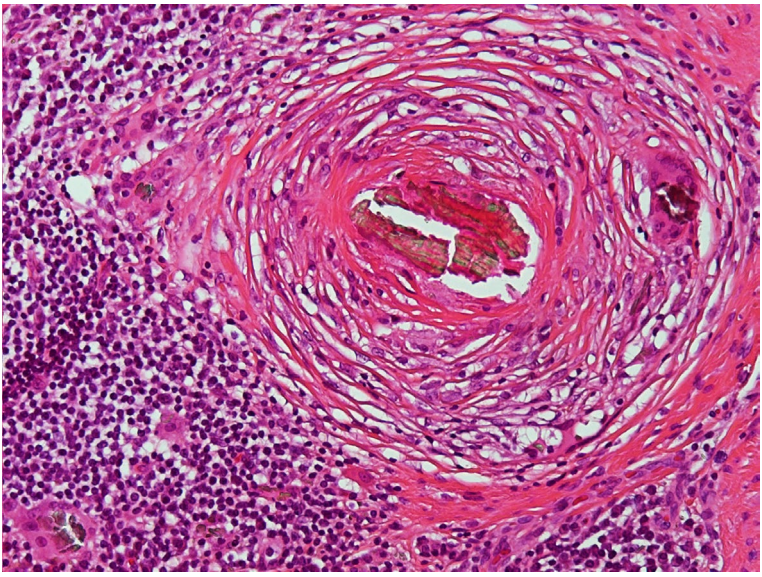

Fig. 10 SLIM type VI. Adverse local tissue reaction: granulomatous pattern. Sarcoid-like granuloma with central large aggregate of greenish/reddish corrosion products, eccentric giant cells containing smaller aggregates, and partial lymphocytic cuffing from metal-on-polyethylene total hip arthroplasty with CoCr dual modular neck implant (H&E, ×200)

2.9 Local Osseous Pathologies (Type VII)

Pathologies of the bone around the acetabular and femoral components of the implant include aseptic loosening/osteolysis, septic loosening/osteolysis (infectious osteomyelitis), osteonecrosis, osteopenia, heterotopic ossification, and periprosthetic fractures [3]. Aseptic osteolysis is the most studied complication, either at implant revision or postmortem [24], [25], [26], [27]. Histologically, it is characterized by the presence of a dense infiltrate of particle-laden macrophages forming a mass with or without central necrosis and increased osteoclastic activity with peri-implant bone resorption (Fig. 11).

Take-Home-Message

- Histological analysis of the SLIM following the expanded international consensus classification and wear particle characterization allows for a more accurate diagnosis of implant failure and can also provide guidance in the determination of a suitable postoperative treatment and follow-up and/or optimization of the therapeutic regimen.
- The SLIM expanded international consensus classification is also useful in the diagnosis of all inflammatory-toxic and hypersensitive-allergic reactions providing detailed information that can be relevant for clinical management.

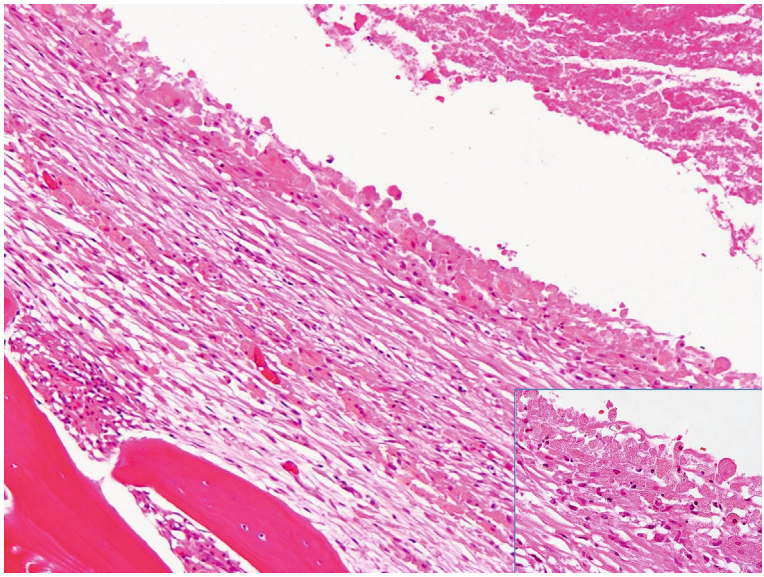

Fig. 11 Aseptic osteolysis. Hip metal-on-metal resurfacing implant: a large amount of particle-laden macrophages involve the bone marrow with formation of a cystic cavity filled with necrotic cell debris in the *upper right corner* (H&E, ×100). At higher magnification, the macrophages contain predominantly globular greenish aggregates of wear nanoparticles (*inset*, ×400)

2.10 Histological Criteria for Periprosthetic Joint Infection

Histological analysis positive for periprosthetic joint infection is a component of periimplant infection diagnosis and constitutes one of three minor criteria as defined at the International Consensus Meeting on Periprosthetic Joint Infection [8]. The method of identification and the threshold value for PMN is at the discretion of the pathologist.

The three most common methods to quantify PMN are the following:

- **1: ≥2 PMN per HPF (×400) in 10 Consecutive HPF**

This PMN quantification method is based on more than 2 PMN per HPF (×400) in the analysis of 10 HPF. The diagnostic value of the score for periprosthetic infections combined with clinical parameters has been validated [28].

- **2: ≥23 PMN in 10 Consecutive HPF (field ×20, Field of View Diameter 0.625 mm)**

This PMN quantification method is based on counting 10 HPF. For each HPF, a maximum of 10 PMN are counted irrespective of the total number exceeding the limit. If there are more than 23 PMN in 10 HPF in total, the diagnosis of a SLIM infection-induced synovitis is made; the sensitivity is 73% and the specificity is 95% [29].

3: ≥50 CD15⁺ PMN in a Single Focal Point of 1 HPF (CD15 Focus Score)

The CD15 focus score is a simple counting algorithm for PMN. This method counts CD15⁺ cells in a single focal point, independent of location, and is based on a specific property of PMN (CD15 expression). Ultimately, this score follows the principle of maximum severity (grading of the worst area), a well-established principle in histological diagnosis that also takes into account the focal nature of the inflammatory infiltrate in the periprosthetic tissue [30].

The PMN count is performed using a ×20 lens magnification in an area or a field size of about 0.26 mm^2 (Fig. 12). With a value of ≥50 CD15 PMN/focal point, in 1 HPF, a bacterial infection can be diagnosed with a sensitivity of 87% and a specificity of 90% [30]. These data validate the CD15 focus score as a method for the histological diagnosis of implant infection and its accuracy is increased by the use of a CD15 quantification software, such as the CD15 Quantifier, VMscope (Berlin, Germany) [30]. Although the quantification of the PMN content remains the gold standard for the histological diagnosis of infection, adjuvant criteria are the loss of lining cell layer, edema, and formation of granulation tissue. In particular, modifications in the structure of the neo-synovial membrane are important in cases of low-grade infection, in which the differential diagnosis with untreated or therapy-resistant inflammatory synovitis of rheumatic disorders in the active phase can also be a challenge, especially on arthroscopic shavings or with limited tissue sampling for frozen section. Usually the presence of hyperplasia of the cell lining layer and of lymphoplasmacytic infiltrate is useful in addressing the correct diagnosis, even when the threshold of the PMN count for low-grade infection is met.

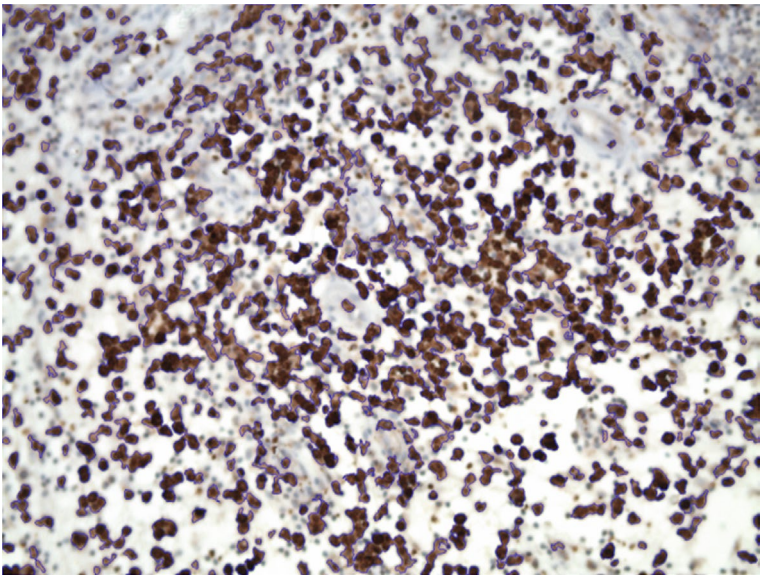

Fig. 12 CD15 focus score in infection-induced SLIM (type II). Case of total hip arthroplasty high-grade infection with positive *E. coli* culture and a CD15 focus score of 485. The cells with a *blue border* represent polymorphonuclear leukocyte (CD15 quantifier mode, field size about 0.26 mm^2)

2.11 Response Patterns for Implant-Associated Allergic/ Hypersensitivity Reaction

Allergic reactions to implant materials as the sole cause of implant failure are a controversial topic in the scientific literature [31], [32]. The prevalence of non-implant-associated metal allergies to nickel is estimated to be around 13% in the general population [33], [34]. Metal allergies to cobalt and chromium are estimated at a much lower rate of 2% and 1%, respectively [33], [35]. Uncommonly, an allergic reaction to a bone cement component, such as benzoyl peroxide, has been implicated [36]. Patients with an implanted joint prosthesis and affected by metal allergies experience more symptoms and complications over time than do patients without metal allergies.

Severe inflammatory reactions with the formation of tissue necrosis as observed in inflammatory pseudotumors associated with corrosion products have not been detected in allergic reactions to implant materials, although the possibility of combined adverse reaction cannot be completely ruled out [31]. Type IV SLIM is predominant in cases diagnosed as allergic tissue reaction to an implant. In these cases, a variable amount of interstitial and/or perivascular lymphocytic infiltrate occurs. The infiltrate can show similarities to the one observed in pseudotumors in the density of the T-cell infiltrate (Fig. 13).

An implant-associated allergic reaction should be suspected and confirmed by clinical tests in SLIM type I and IV synovitis in the presence of interstitial and perivascular T-cell lymphocytic infiltrate of variable intensity with or without the presence of eosinophilic infiltrate and increased number of mast cells.

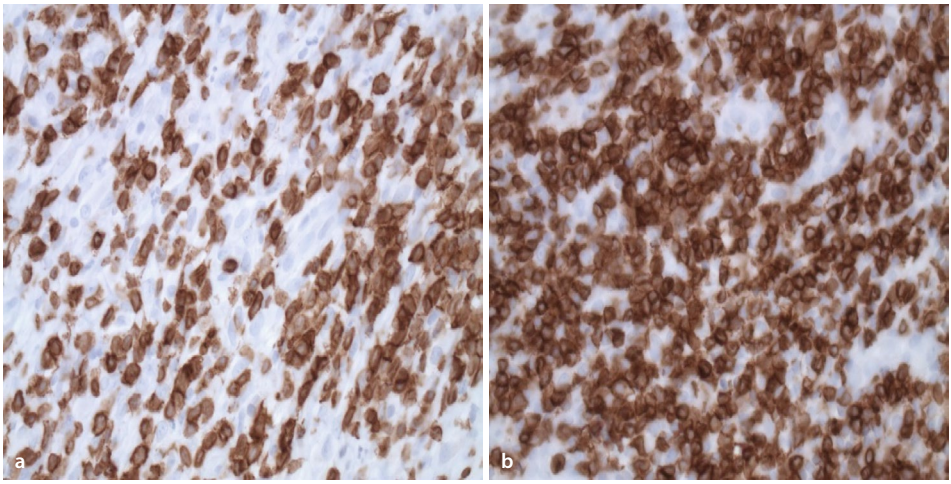

Fig. 13 Adverse reactions with T-cell CD3$^+$ lymphocytic infiltrate. T-cell rich (CD3$^+$) lymphocytic infiltrate in non-metal-on-metal (MoM) total hip arthroplasty with verified nickel allergy (**a**) and in MoM resurfacing hip arthroplasty implant (**b**). In both cases, no coexisting B cells were identified. T-cell values were 399 in **a** and 577 in **b** measured by CD3 Quantifier software (indirect immunoperoxidase reaction, ×300)

2.12 Response Patterns for Implant-Associated Toxic Inflammatory/ Hypersensitivity Reaction

Hip prostheses with a MoM-bearing surface either in hip resurfacing arthroplasty (HRA) or in total hip arthroplasty (THA) and non-MoM-bearing surface, such as metal-on-polyethylene (MoP), ceramic-on-polyethylene (CoP), and ceramic-on-ceramic (CoC) with cobalt-chromium (CoCr) dual modular neck (DMN), and MoP-bearing surface with various head–neck taper configurations can show ALTR characterized by the formation of a periprosthetic soft tissue reaction called a pseudotumor [22]. The pseudotumor can extend to an adjacent bursa and can be defined as "a mass of variable size formed by the thickening and invagination of the joint pseudocapsule and neo-synovial membrane with frequent papillary or polypoid configuration with absence or presence of a layer of necrosis/infarction of variable thickness filled with a variable amount of synovial fluid ranging from serous to creamy consistency."

The main histological patterns were described in the section on SLIM type VI. All patterns can show bone involvement of particle-laden macrophages with or without formation of cavities (osteolysis) and/or reactive lymphocytic aggregates [4], [19], [20], [22], [37]. A layer of tissue necrosis/infarction of variable thickness can be present in patterns 2 and 3 but it is absent in pattern 1.

Macrophagic-mediated femoral and/or acetabular osteolysis can become the predominant type of ALTR with the longer time of implantation in THA implants and with formation of corrosion products; in these cases the prevalence and the modalities of longitudinal follow-up are to be determined [4]. Distinct quantitative and qualitative histological differences in various classes of implants associated with ALTR have been described [4] [20].

Immunohistochemical studies of cases of ALTR of MoM THA with MAS and non-MoM THA with DMN have shown the presence of $CD68^+$ and $CD163^+$macrophages, $CD3^+$ T cells with $CD4^+$ and $CD8^+$ subsets in various proportions, Th1 (t-bet^+), Th2 (GATA-3^+), and Treg ($FOXP3^+$) lymphocytes, and $CD117^+$ mast cells that are more numerous in the presence of eosinophilic infiltrates and/or lymphocytic germinal centers [20]. Lymphocytic infiltrate has been characterized in detail in MoM implants and has been subdivided into three distinct groups: (1) diffuse T-cell infiltrate without aggregates; (2) T-cell infiltrate with aggregates; (3) mixed T-cell and B-cell infiltrate with aggregates and formation of germinal centers [23]. Moreover, the close relationship between $CD3^+$ T-cell lymphocytes and $CD1^+$ and S-100^+ dendritic stromal cells (Fig. 14) has not been studied yet, and its contribution to adverse reactions is still undetermined.

The elucidation of the pathogenic mechanism(s) of the reaction, either of allergy/hypersensitivity to or toxicity of the wear particulate material or the mixed material is complicated by the following variables: (1) changes in the tribological lubrication due to thickening of the synovial fluid by macrophagic necrotic debris with possible acceleration of the wear process [4]; (2) release of partially digested/oxidized secondary nanoparticles from the necrotic macrophages with cell membrane coating [4]; (3) direct erosion of the implant metallic surface by cellular mechanisms [38], [39]; (4) coating of nanoparticles by proteins of the synovial fluid possibly acting as hapten for an allergic reaction [40], [41];

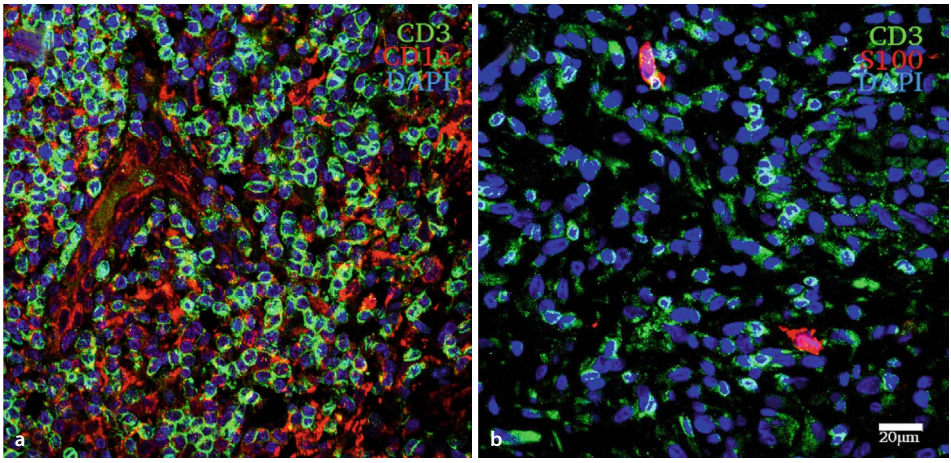

Fig. 14 Confocal laser scanning microscopy (SLIM type I). $CD3^+$ T lymphocytes (*green*) that are colocalized with dendritic cells (*red*) in **a** (CD1a stain) and in **b** (S100 stain). A functional interaction of these cells due to their spatial proximity is postulated. Image material prepared in cooperation with the Department of Anatomy and Molecular Embryology of the Ruhr University Bochum, Germany (DAPI stain, ×400)

(5) comorbidities with marked synovial inflammatory infiltrate at time of implantation (time zero), i.e., rheumatic disorders.

In conclusion, when a marked lymphocytic infiltrate is observed histologically in the periprosthetic tissue and especially in the absence of a significant implant wear (SLIM type IV), the possibility of an allergic reaction must be considered. In cases of a mild lymphocytic infiltrate, the differential diagnosis of functional causes, biomechanical causes, and prosthesis-associated arthrofibrosis versus allergic reaction should be discussed reviewing pertinent clinical and laboratory data [42].

Take-Home-Message

- Adverse local tissue reactions associated with metallic implant wear (corrosion products and conventional metallic particles) include immunologically mediated reaction secondary to particle toxicity and/or hypersensitivity/allergy to metallic particles/ions.
- The histopathological findings must be interpreted in the context of clinical, allergological, imaging, and biomechanical data.
- With high-grade lymphocytic infiltrate in the presence or absence of tissue necrosis/infarction, the diagnosis of an implant-associated immunological-allergic reaction and/or toxic reaction must be considered in the differential diagnosis.
- With low-grade lymphocytic infiltrate, the diagnosis of an implant-associated immunologically mediated hypersensitivity/allergic reaction should be considered in the differential diagnosis.

2.13 Particle Algorithm

The identification, systematic analysis, and characterization of wear particulate components of implant materials as well as their differentiation from non-implant-generated particulate materials are very important in providing information useful for identifying causes of joint implant failure. Ideally, the analysis should be performed with knowledge and examination of the removed implant components and of the operative report with technical information on the implant and the manufacturer, which should be included in the macroscopic description of the specimen and be part of the final report. These particles can be characterized at standard light microscopy examination using as a guide the standardized particle algorithm (Fig. 15), which is currently subject to revision [43]. This particle algorithm is based on previously published particle-defining criteria [44], [45]. It can be used with the SLIM classification to complement the clinical, allergological/immunological, microbiological, radiological, and biomechanical data for the identification of the pathogenic mechanism(s) of implant failure of specific implant classes and/or configurations [6]. The particles are characterized at light microscopy using paraffin sections conventionally stained with hematoxylin and eosin (H&E). They are classified according

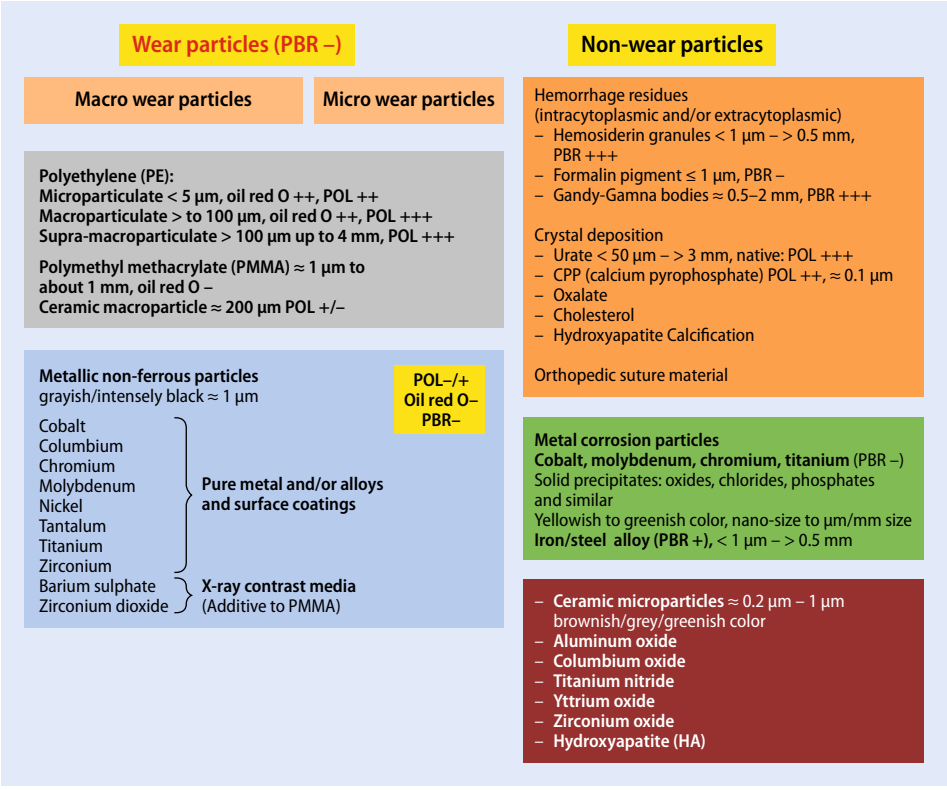

Fig. 15 Particle algorithm of neo-synovial membrane

to their morphological characteristics (size, shape, color) with the resolving power limited to the size of about 1 µm (although aggregates of smaller particles can be identified without specific characterization). Adjuvant tools such as polarization optical analysis for birefringent particles and histochemical analysis with special stains (e.g., oil red O stain, Prussian blue reaction), can also be used when necessary. Quantitative analysis can be performed with a semiquantitative numerical score for particle content and has been described and used in the past [46], [47]; its accuracy is, however, variable even when using image analysis software for automated counting when the particulate material is in the sub-micron and nano-size range and in cases of complex wear with multiple materials engulfed by the macrophages that cannot be reliably measured at light microscopy examination.

For particle differentiation and element analysis, physical methods such as energy-dispersive X-ray spectroscopy (EDS) or Fourier transform infrared microspectroscopy (FTIR) enable a more precise identification of particular components [18]. More recently, nano-analysis has been applied for the identification of metallic nanoparticles using glutaraldehyde-fixed, resin-embedded tissue blocks for toluidine blue-stained histological semi-thin sections. These are used to select appropriate areas for back-scatter scanning electron microscopy (BSEM) or BSEM-EDS and element mapping and preparation of ultrathin sections (unstained or lead-uranium stained) for transmission electron microscopy (TEM), TEM-EDS, TEM-EDS mapping, and X-ray diffraction spectrometry (XRD) [48], [49].

Take-Home-Message

- The particle algorithm provides an easy and reliable guide for the identification of particulate material in the periprosthetic tissue. It is useful for identifying mechanisms of failure of the joint prostheses in the context of clinical, allergological, microbiological, histological, radiological, and biomechanical findings.

2.14 Characterization of Wear Particles

The study of wear particles and their interaction with macrophages is a fascinating and ever-evolving field that involves a large number of specialties of medicine and other disciplines. However, the correct identification of the particulate wear material is the first, essential step of a very complex and in-depth analysis to provide clues of the host response. The main types of particles are herein described and illustrated as a practical aid for their classification at light microscopy examination.

Polyethylene Particles

The characterization of polyethylene particles is important because osteolysis has been recognized as being a major complication and cause of failure in joint replacement based on inserts of ultrahigh-molecular-weight polyethylene (UHMWPE). Unlike other

implant materials (i.e., ceramic, metal), polyethylene particles can be identified without much effort based on their characteristic appearance at light microscopy and under polarized light and on their histochemical properties, although quantitative assessment of small particles is more difficult and less accurate. Occasionally, the differential diagnosis with birefringent suture material can be challenging, especially if the material breaks down into filamentous fragments, mimicking the structure of polyethylene (PE). The dimension and shape of PE particles vary from sub-micron and needle-like to several microns or even millimeters and clasp-like. Their morphological features depend in large part on the type of polyethylene used and its processing method. UHMWPE wear is largely macroparticular, while highly cross-linked polyethylene (HXLPE) is predominantly microparticular. However, several factors can influence the amount and size of the wear particles independently from the structure of the material: (1) type of sterilization process (gamma radiation, ethylene oxide, gas plasma, postirradiation thermal treatment); (2) packaging material; (3) hardness of the femoral head material; (4) third-body wear resistance [50]. The particle algorithm provides the following classification of particles according to size: *microparticles*, phagocytized by macrophages and ≤5 μm; *macroparticles*, phagocytized by multinucleated giant cells and ≤100 μm; and *supra-macroparticles*, ≥100 μm lined by giant cells and with an extracellular location in some cases [43].

▪ Microparticles (<5 μm)

At conventional light microscopy (H&E staining), PE microparticles can only be detected with difficulty, especially for a semiquantitative analysis. Their identification can be enhanced using special staining methods and in particular the oil red O stain [45]; however, the stain is nonspecific and must be interpreted carefully in the presence of other wear materials, such as metallic corrosion products in MoP implants (◘ Fig. 16a and b).

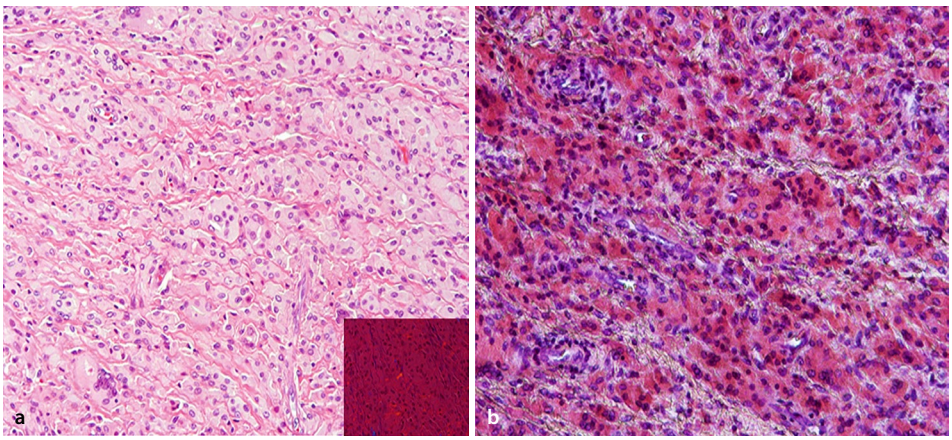

◘ **Fig. 16** Polyethylene microparticles. **a** Macrophages and occasional giant cells show pale gray cytoplasm (H&E, ×200) containing birefringent globular and needle-shaped material under polarized light (*inset*, ×400). **b** The macrophagic cytoplasm stains red with oil red O stain, enhancing the particle content (×200)

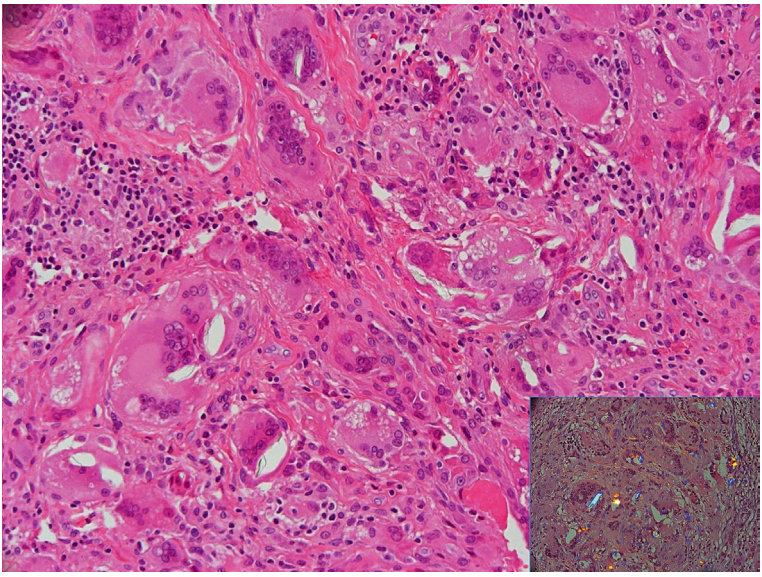

Fig. 17 Macroparticulate polyethylene. Polyethylene macroparticles in numerous multinucleated giant cells (H&E, ×200), birefringent under polarized light (*inset*, ×400)

Macroparticles (>5–100 µm)

At light microscopy and polarization optical analysis, PE macroparticles are polymorphic structures with a distinctive appearance that are localized in multinucleated foreign-body-type giant cells (Fig. 17).

Supra-macroparticles (≥100 µm)

The PE particles are noticeable for their large size, ranging from ≥100 µm up to more than 1 mm, and are visible at low-power magnification (×10) and even with the naked eye. The shape of the supra-macroparticulate polyethylene particles (Fig. 18) is variable ranging from polygonal to long, clasp-like. The localization of the supra-macroparticulate polyethylene particles varies with placement in multinucleated foreign-body type giant cells and/or in viable or necrotic extracellular matrix [43]. The term "PE vacuole" has been suggested for supra-macroparticulate PE that is extruded from the tissue [43]. PE vacuoles can be up to several millimeters in length. The vacuole-shaped spaces corresponding to the particle shape are lined by fibroblasts and macrophagic and multinucleated foreign-body-type giant cells. The fibroblasts in particular are aligned along the surface of the vacuole. They have been observed predominantly in the periprosthetic tissue of knee joint implants. The cause(s) of failure should be determined by combined clinical, biomechanical, and PE oxidative state analysis with histological correlation [43].

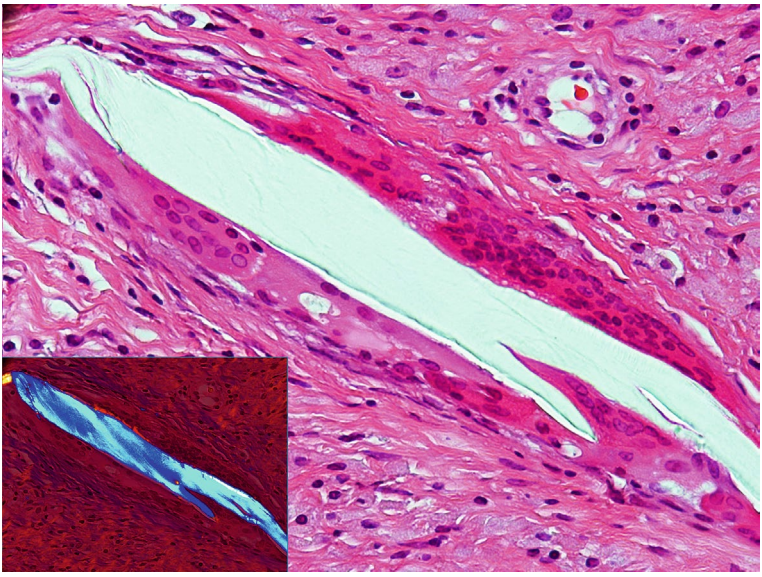

Fig. 18 Polyethylene supra-macroparticle with adjacent multinucleated giant cells (H&E, ×400) with birefringence under polarized light in the *inset* (×400)

Take-Home-Message

- The analysis of PE debris is important because it is still a main cause of osteolysis, a major cause of revision of joint implants, and should be associated with the examination and technical description of the implant, included in the pathological final report.
- The basic subdivision of the PE debris into micro-, macro-, and supramacro-particulate is proposed to be correlated with the biomechanical analysis of the implant and the oxidative state of the material.
- The occurrence of supra-macroparticles in PE degradation should be reported as a major failure of the insert; the cause of its occurrence should be determined for each implant with detailed biomechanical analysis to differentiate among material oxidative degradation and mechanical failures such as misalignment, impingement, dislocation, rim fractures, and third-body wear.

Metallic Particles

The subject of metallic wear particles is complex because of the various types of reactions that can lead to their formation and can be subdivided into two broad categories: the non-ferrous conventional metallic particles generated by abrasion/edge loading and the corrosion metallic particles generated by electrochemical reactions such as tribocorrosion at the bearing surface of MoM implants and mechanically assisted crevice/fretting corrosion at the trunnion junctions.

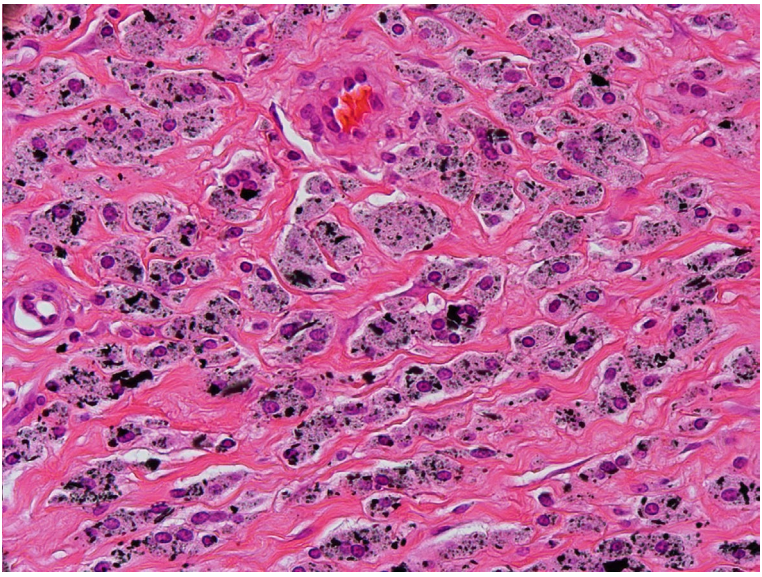

Fig. 19 Conventional metallic particles. Macrophages containing intense black, round to polygonal, intracytoplasmic metallic microparticles from failed metal-on-polyethylene hip implant (H&E, ×400)

Non-ferrous Conventional Metallic Particles

Non-ferrous metals and their alloys are increasingly used in arthroplasty, whereas ferrous metal alloys (e.g., steel) are used considerably less often. Non-ferrous metal alloys usually contain titanium, tantalum, aluminum, vanadium, cobalt, molybdenum, chromium, niobium, and nickel in various combinations and alloys. The presence of metallic fixation devices, such as acetabular metallic screws, should be known and be assessed at the time of histological examination because a breakdown of these elements can generate metallic debris indistinguishable at light microscopy from the one derived from the implant component(s). Conventional metallic wear particles generated by abrasion vary in color from gray to black, have a mean diameter ranging from about 0.1 µm to 100 µm [45], and vary in shape from round to needle-like/polygonal with sharp edges (Fig. 19). Metal particles exhibit no or only minimal peripheral birefringence. Birefringence of particles in the macrophages can be observed in the presence of microparticulate PE admixed to metallic wear debris. Because these metallic particles are non-ferrous, they cannot be visualized with the Prussian blue reaction (PBR).

Non-ferrous Corrosion Metallic Particles

MoM-bearing surfaces and metallic trunnion surfaces can be sources of wear metallic corrosion products generated by electrochemical reactions [51]. The occurrence and amount of this type of wear are multifactorial, including implant design, positioning, and the level of patient activity. Wear particles produced at the bearing surface of MoM hip implants, either HRA or THA, by tribocorrosion are usually composed of Cr-Co-Mo,

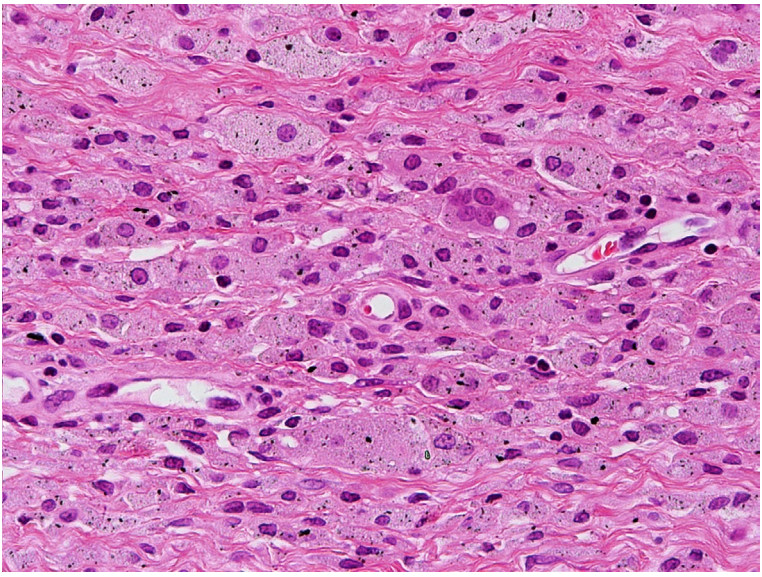

Fig. 20 Combination of conventional and corrosion metallic particles. Macrophages containing a mixture of Cr-Co-Mo microparticles observed as pale green globular aggregates of nanoparticles generated by tribo-corrosion and Cr-Co-Mo gray–black, needle-shaped to polygonal, sharp-edged, microparticles generated by edge loading in a case of metal-on-metal hip resurfacing arthroplasty (H&E, ×400)

are of nano-size ranging from less than 10 nm to 100 nm [48], [52], and can be mixed to conventional metallic particles of similar composition but of larger size generated by edge loading (Fig. 20). Corrosion particles appear greenish/yellowish and globular in the phagosome/lysosome complex of the macrophages, originally described as droplet-like cytoplasmic inclusions of wear products of uncertain composition [53] (Fig. 21 and b). A more complex mixture of particles appears in the MoM LHTHA implants, in which wear particles generated at the neck/metallic adapter sleeve interface by fretting/crevice corrosion can also be present with the addition of titanium from the stem as aggregates of nano-size of micron-size particles ranging from <1 μm to >500 μm (Fig. 22). These large aggregates often show a multilayered structure of greenish/black/reddish material that can contain blood products positive to PBR [4], [20]. In implants with non-MoM-bearing surface, the corrosion products are generated at the neck/stem contact surface in implants with CoCr DMN and at the metallic head/neck taper surface as large aggregates that break down in the joint cavity into smaller aggregates phagocytized by the macrophages. Large aggregates of corrosion products lined by giant cells can also be generated at MoM interfaces of fixation devices, such as metallic plate/metallic screws (Fig. 23).

Hemosiderin Particles with Iron Content

Hemosiderin particles containing iron of variable size and quantity can be present in the periprosthetic soft tissues. The majority of these are derived from degeneration of hemo-

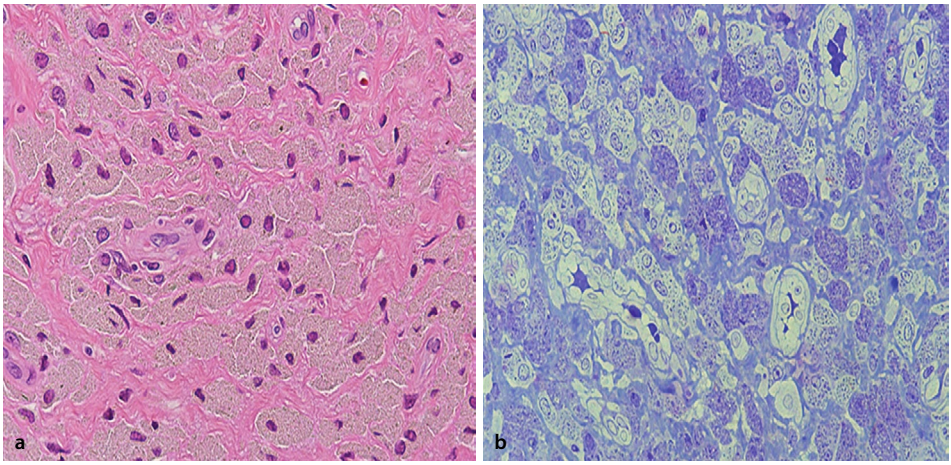

Fig. 21 Macrophagic infiltrate containing globular aggregates of metallic nanoparticles generated by tribocorrosion at the bearing surface of a metal-on-metal hip resurfacing arthroplasty implant (time of implantation 60 months) in conventional section (**a** H&E, ×400) and semithin section for electron microscopy preparation (**b** Toluidine blue, ×400)

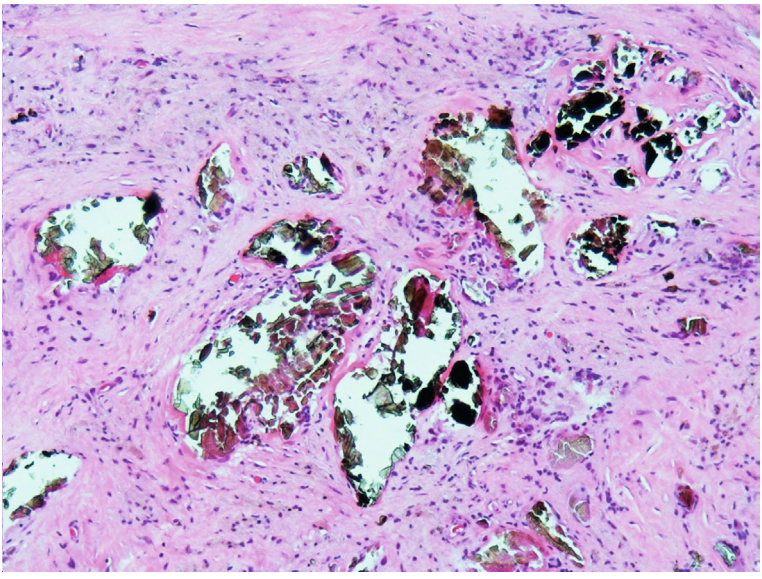

Fig. 22 Numerous aggregates of wear particles generated by fretting/crevice corrosion from metal-on-metal LHTHA with metallic adapter sleeve (time of implantation 91 months) as sheet-like greenish/black/reddish deposits in periprosthetic capsule (H&E, ×100) with distinct laminar structure (*inset*, ×400)

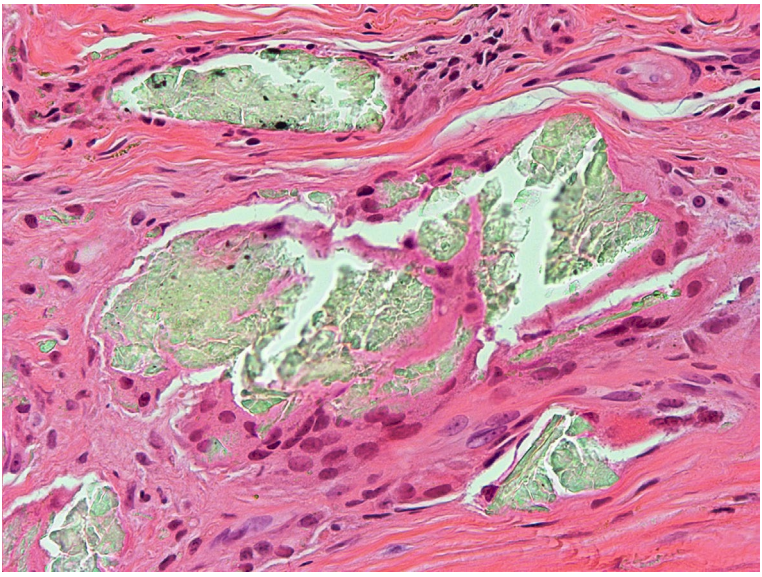

Fig. 23 Large aggregates of corrosion products generated from a metallic blade–plate/metallic screws fixation device (H&E, ×400)

globin due to hemorrhage secondary to mechanical complications (e.g., patellar malfunction and instability, dislocation(s), periprosthetic fracture). They are easily detectable with the PBR stain, which is blue in their presence (Fig. 24a and b). The stain is also useful to differentiate between fine globular hemosiderin particles and globular aggregates of nano-size particles of corrosion products or fine ceramic particulate debris that can have a similar color on H&E stain.

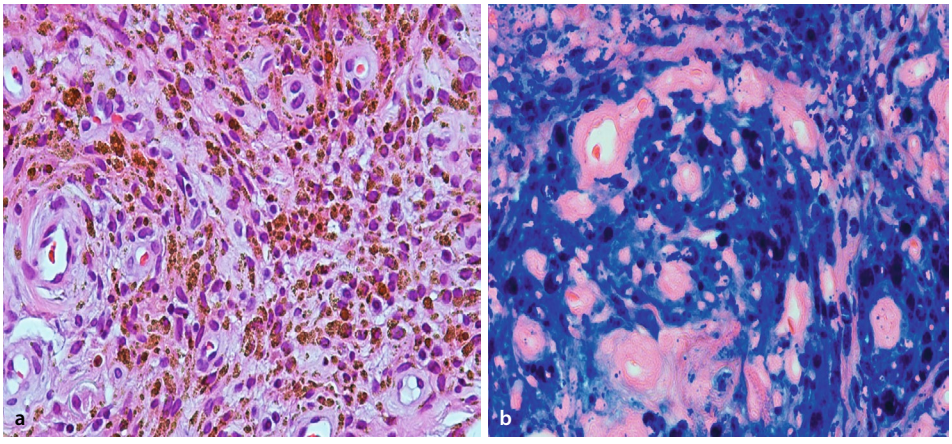

Fig. 24 Hemosiderin particles. Macrophagic infiltrate containing hemosiderin particle with iron content. Deposits range in shape from fine to coarse granules, gold brown in **a** (H&E, ×400) and blue in **b** (Prussian blue, ×400)

Ceramic Particles

Ceramics are generally employed in joint replacement arthroplasty as combinations of CoPin either hip or knee implants or CoC-bearing surfaces in hip implants only. They are classified as:

1. Oxidized ceramics, composed of aluminum oxide ceramic (Al_2O_3), zirconium dioxide ceramic (ZrO_2), or alumina matrix composite (mixed oxide ceramic) with components such as yttrium oxide (Y_2O_3), strontium oxide (SrO), or chromium oxide (Cr_2O_3)
2. Non-oxide ceramics such as silicon nitride (Si_3N_4)
3. Hard coating on metals such as titanium nitride (TiN)
4. Surface modifications of metals, such as a zirconium alloy with 2.5% of niobium through surface oxidation by thermal diffusion
5. Calcium phosphate ceramics such as hydroxyapatite and tri-calcium phosphate [54], [55]

Wear-induced ceramic particles occur in sizes ranging from nano-size up to several microns [45], [56]. In cases of fractured ceramic components, macroparticles of up to several millimeters in size have been detected. The shape in the SLIM varies from round to polygonal with sharp edges. The particles exhibit only peripheral, weak birefringence and are highly variable in color, ranging from yellowish-brown, greenish, to gray–brown or intense black, and metal-like depending on the type of ceramic material (Fig. 25, Fig. 26, Fig. 27). In particular, the differentiation between ceramic and metallic debris and/or corrosion products can be very difficult or impossible at conventional microscopic examination especially if mixed in the macrophagic cytoplasm, and elemental composition analysis is required for definite characterization.

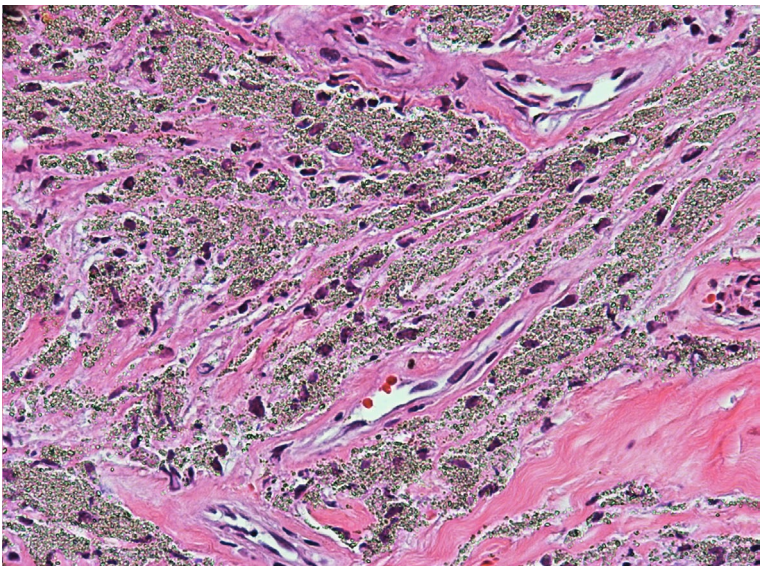

Fig. 25 Ceramic particles. Macrophagic infiltrate containing particles of ceramic debris in a case of a ceramic-on-ceramic hip implant failure secondary to rupture of alumina ceramic acetabular liner (H&E, ×400)

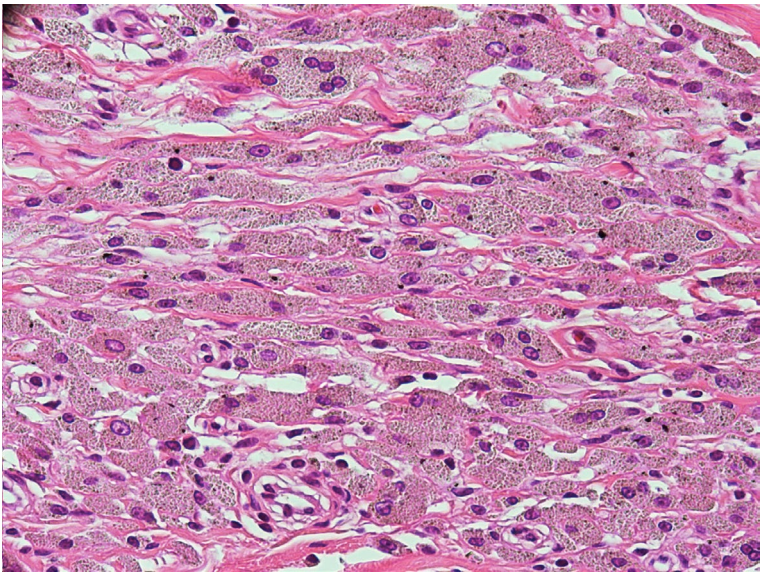

Fig. 26 Ceramic particles. Ceramic particulate material is present in the macrophagic infiltrate as brown to greenish, globular to irregular cytoplasmic particles in a case of a ceramic-on-polyethylene hip implant failure secondary to recurrent dislocation, with alumina–zirconia composite femoral head (H&E, ×400)

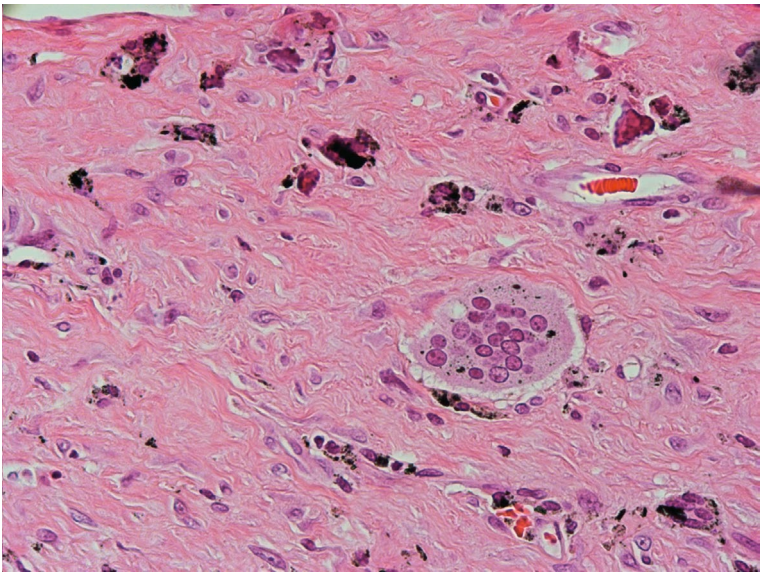

Fig. 27 Ceramic particles. Ceramic particulate material is present in macrophages and a giant cell in a failed metal-on-polyethylene hip implant with oxidized zirconium metallic femoral head. Ceramic particles of oxidized zirconium cannot be distinguished from conventional metallic particles at light microscopy examination (H&E, ×400)

Orthopedic Cement Particles (Polymethyl Methacrylate)

Orthopedic cement is a polymer system composed of methyl methacrylate polymerized by the addition of an initiator and an accelerator. Other additives such as X-ray contrast agents (zirconium dioxide or barium sulfate), benzoyl peroxide, *N,N*-dimethyl-*p*-toluidine, and antibiotics (e.g., gentamicin) can be added in order to achieve optimal use, inclusive of radiological examinations.

Orthopedic cement particles are usually dissolved during conventional histological tissue processing and are no longer directly visible at light microscopy examination. The optically empty space previously occupied by the cement is a mostly polycyclic, vacuole-like cavity usually lined by multinuclear giant cells. Only the residues of additives (barium sulfate or zirconium dioxide) to the cement are visible in the conventional histological sections. Barium sulfate is usually present in the form of mostly intensely blackish, acinar aggregates that are predominantly located at the periphery of the vacuoles (◘ Fig. 28).

In the case of focal, microscopic deposits with minimal inflammatory reaction, bone cement particles can represent an incidental finding and not the cause of a pathologic reaction leading to implant failure, as in cases with florid macrophagic and giant cell reaction, chronic inflammatory infiltrate, and necrobiosis. Of interest is the presence of numerous particles of orthopedic cement contrast agent in the macrophagic infiltrate in cases of third-body wear with cement particle grinding that may lead to implant aseptic loosening (◘ Fig. 29).

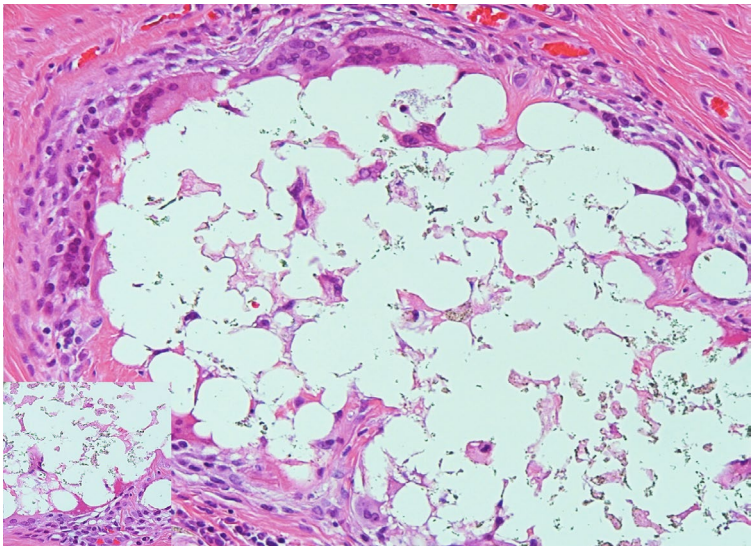

◘ **Fig. 28** Polymethyl methacrylate (PMMA) orthopedic cement. Chemically dissolved PMMA appears as oval to polycyclic, vacuole-like cavities surrounded by multinucleated giant cells. The bone cement additive (X-ray contrast medium), zirconium dioxide in this case, is visible in the *inset* (×400) as small aggregates of greenish, globular particles (H&E, ×200)

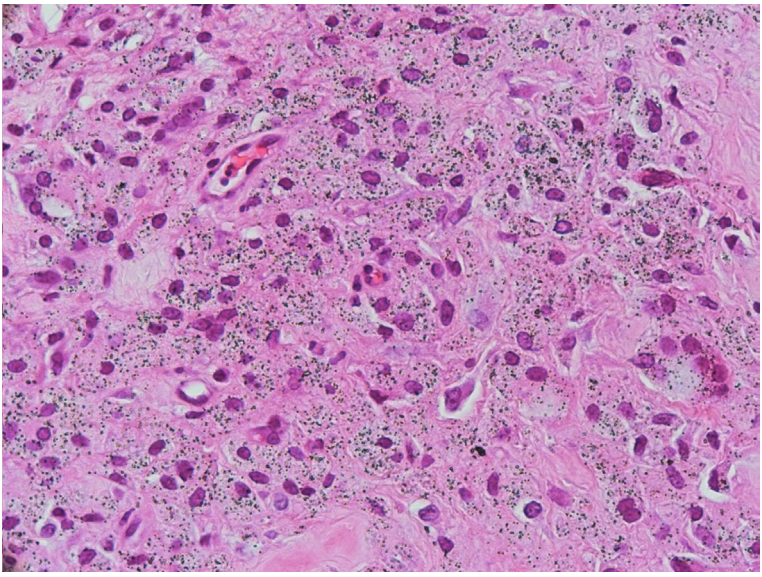

Fig. 29 Polymethyl methacrylate orthopedic cement. Florid macrophagic infiltrate containing numerous particles of zirconium dioxide in a case of unicompartmental knee implant failure secondary to third-body wear (H&E, ×400)

3 Clinical Approach to Synovial-Like Interface Membranes

Wear particles are one of the main causes of prosthesis loosening. SLIM allows us to shed light on the processes occurring at the level of the interaction between the particle and the soft tissue on the implant interface. Information received via microscopy and some kinds of histological analyses can be compared with radiological findings and intraoperative tissue conditions.

The influence of implant positioning and neck-on-liner impingement on prosthesis loosening could be clarified by examining the SLIM. There are numerous data concerning the influence of implant component malposition on the survival rate of implants, but without an exact explanation of how it works. Controlling the pathogenetic triggers of osteolysis can be used for the prophylaxis of implant loosening.

The optimum size of the femoral ball head for hip implants is not defined. There are several pros and cons concerning heads of greater diameter and smaller ones. However, there is a lack of information in the literature about the association between the head diameter and bone osteolysis.

Research on SLIM can offer additional information on the pattern of bearing wear and the comparative performance of various types of materials. Such information can help manufacturers improve materials that are currently available on the market leading to better clinical outcomes for partial and total joint arthroplasties.

4 Standardized Collection and Processing of Periprosthetic Tissue Samples

4.1 Clinical Data

It is essential that adequate clinical history and data are accessible to the pathologist in order to provide the most accurate pathological report. These data should include:

- Demographic details (age, sex, body mass index)
- Clinical history with relevant comorbidities
- Type of prosthesis and material(s) of each component, cemented/noncemented
- Design of previous prostheses in case of previous multiple revision surgeries
- Polyethylene wear volume (measured using 3D scanning of retrieved implant or at least assessment of presence of bulk wear, e.g., impingement-induced wear or detached owing to massive wear macroparticles)
- Time of implantation at time of revision
- Clinical studies (imaging, allergological tests, microbiological analysis)

4.2 Tissue Collection

The modalities of a standardized tissue collection of periprosthetic tissue described here are based on the criteria reported in the literature [8], [20] and on the interdisciplinary cooperation in Working Group 11 – Implant Intolerance – of the German Society for Orthopedics and Orthopedic Surgery [57].

General Considerations

As a general rule, the histological diagnosis is more accurate and clinically meaningful when tissue samples of adequate size are collected, and this is especially true for inflammatory diseases, where the findings can be focal or of variable intensity in different areas. Therefore, the number of tissue samples collected for soft tissue pathology of joint prostheses should vary from a minimum of three to six or more, according to the size of the joint and the extent of the reaction. Additional samples should be provided for the osseous tissue adjacent to the implant and especially in cases of osteolysis, if feasible. In any case, the locations and size of any tissue sampling must be left at the discretion of the operating surgeon so as not to jeopardize the optimal outcome for the patient. The following general areas should be sampled:

- Close to the prosthesis (SLIM/periprosthetic membrane).
- Interface side of the tissue samples taken should be marked using sutures.
- Far from the prosthesis (SLIM/periprosthetic membrane) muscles interface, muscle-synovial-like membrane interface (Fig. 2).
- Osseous tissue adjacent to the implant (optional).

For the hip joint, the following additional collection sites can be used: head–neck junction, proximal osteolytic gap between stem and bone, and the retroacetabular area.

For each collected tissue sample, the patient's identification data and the anatomical location must be recorded on the label of the designated container before submitting it to pathology.

Tissue Collection at Implant Revision Surgery

At revision surgery, periprosthetic tissue should be collected through careful dissection with a scalpel blade without using cautery, which causes tissue artifacts and makes it unsuitable for immunohistochemical studies and eventual electron microscopy and/or RNA analysis (Fig. 30a, b). In cases of advanced ALTR with the presence of necrosis, sampling should include the interface between the necrotic tissue layer and the adipose tissue where the inflammatory infiltrate is present. The use of forceps should be discouraged in these cases because of separation of the inner necrotic layer from the viable adjacent tissue, providing inadequate material for histological examination even with multiple samples. Knowledge of the implant and location(s) where the significant wear particles are generated is also important because the reaction can be more marked in sites where the particulate material is embedded in the neo-synovial membrane. Guidance provided by MRI and/or ultrasound studies to select the most reactive areas is useful when available [58], [59].

Tissue Collection with Implant in Place

Arthroscopy

Each tissue sample collected during standard joint arthroscopy (three to six specimens) should have a diameter of at least 1 cm and be representative of the most affected areas (Fig. 31).

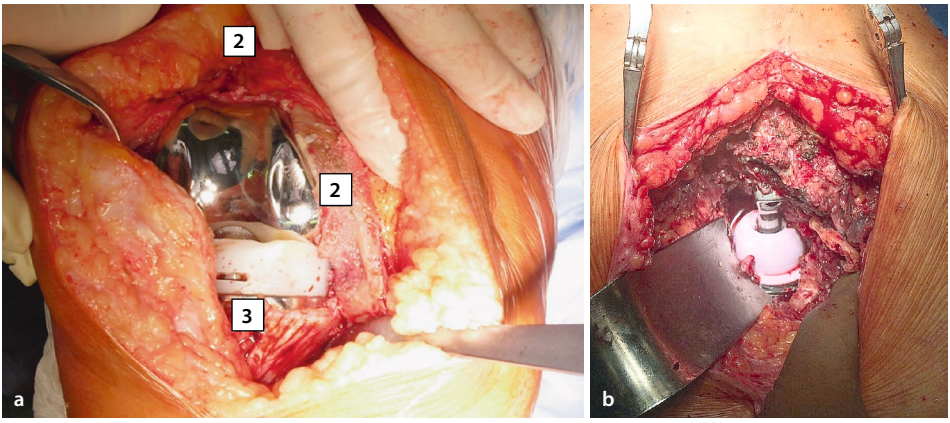

Fig. 30 **a** Tissue collection during implant revision in a case of total knee arthroplasty: (*1*) SLIM/periprosthetic membrane "close to the prosthesis," around the prosthesis shield; (*2*) SLIM/periprosthetic membrane "far from the prosthesis," upper recess; (*3*) osseous tissue, close to the prosthesis. **b** Tissue collection during implant revision in a case of total hip arthroplasty: (*1*) SLIM/periprosthetic membrane "close to the prosthesis," around the prosthesis shield; (*2*) SLIM/periprosthetic membrane "far from the prosthesis"; (*3*) osseous tissue, "close to the prosthesis"

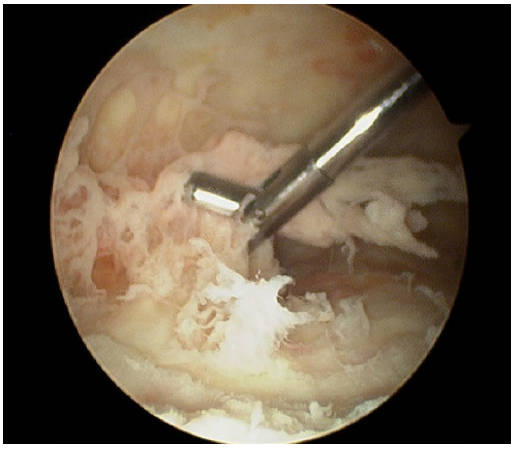

Fig. 31 Collection of synovial samples during arthroscopy with prosthesis in place

Retrograde Synovial Biopsy

In addition to arthroscopy, synovial tissue can also be collected by a minimally invasive technique using a biopsy forceps (Retroforce, Karl-Storz GmbH) as recently described [60]. In brief, the instrument is inserted into the joint cavity through a small 2-mm incision under local anesthetic and the intra-articular position is checked by aspirating fluid or under visual control (Fig. 32). After opening the forceps, the instrument is withdrawn until resistance is felt. The handles of the forceps are closed and a tissue punch sample is collected with subsequent retrieval of the forceps from the joint. The procedure can be repeated several times through the same opening to obtain biopsies from different loca-

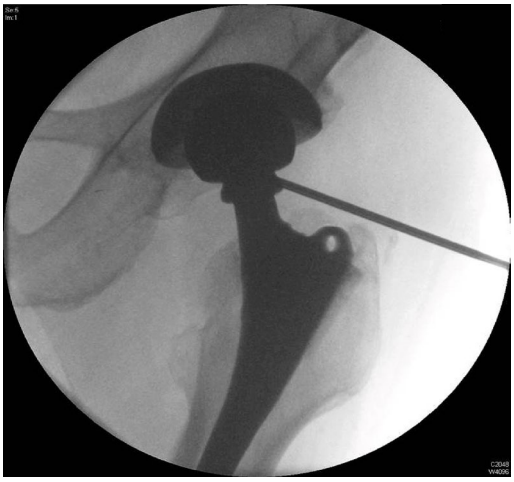

Fig. 32 Retrograde synovial biopsy following hip arthroplasty with suspected wear-induced implant failure. The instrument is advanced under fluoroscopy with local anesthetic up to the joint, opened, and withdrawn back to the synovial-like interface membrane

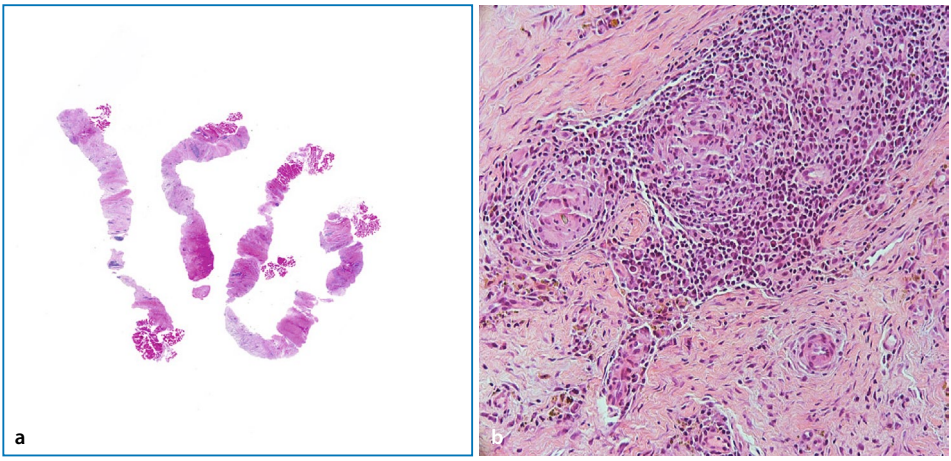

Fig. 33 Core needle biopsy. Cores of periprosthetic neo-capsular tissue (**a**) and adverse local tissue reaction with sarcoid-like granulomatous pattern (**b**) and giant cell containing corrosion product aggregate particle (*white arrow*) in failed metal-on-polyethylene implant with CoCr dual modular neck (H&E, ×200)

tions around the joint. This procedure is particularly well suited to knee and hip joint prostheses but can also be used for shoulder and ankle joints.

Ultrasound-Guided Fine Needle Synovial Biopsy

Another minimally invasive procedure that can also provide useful information is fine needle core synovial biopsy performed under ultrasound guidance. In brief, ultrasound is performed prior to the biopsy procedure and assessed for the presence of effusion, synovial thickening, soft tissue mass, and fluid collection decompressing into the great trochanteric bursa through dehiscence of the capsule. Correlation with the MRI study is also made, if available, before the procedure. Biopsies are performed in the most affected areas with multiple passes using a 14-gauge core biopsy system with cores immediately fixed in buffered 10% formalin solution and sent to pathology (Fig. 33a and b).

Core bone biopsies can also be performed during surgery to sample areas of osteolysis that would be difficult to remove without creating a large gap in the osseous surface.

4.3 Tissue Submission to Pathology During Arthroscopy and/or Revision Surgery

A flowchart for periprosthetic tissue collection and its applications in the pathological examination is provided in Fig. 34.

Fresh Tissue

Fresh tissue retrieved from the operating room sterile area as soon as possible and kept on ice is increasingly replacing the traditional collection of formalin-fixed tissue, allowing for

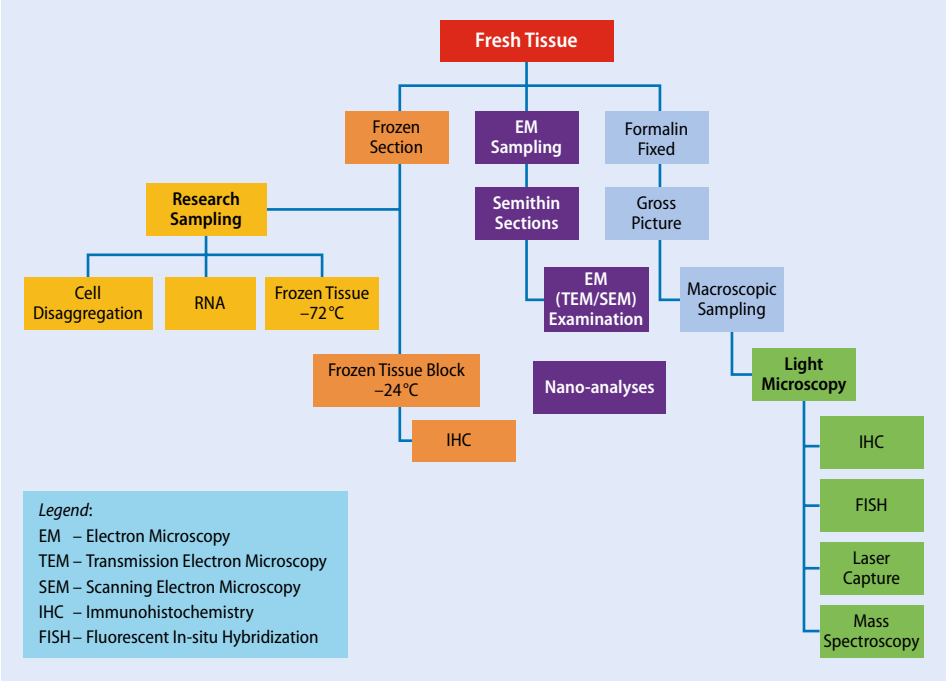

Fig. 34 Pathological examination of implant revision specimens. Flowchart of the collection of fresh tissue illustrating the major methods of its analysis by multidisciplinary laboratories

the use of molecular technology and for correlation with the histological examination. The tissue is sent to pathology and after macroscopic examination a frozen section is performed on the most representative sample to assess viability and cell composition. When feasible, a representative tissue sample adjacent to the one examined for frozen section can be collected for RNA isolation and cell disaggregation, fixed in glutaraldehyde for electron microscopy examination, and snap frozen in liquid nitrogen for wear element analysis by inductively coupled plasma atomic emission spectroscopy (ICP-AES), synchrotron micro-X-ray absorption spectroscopy (XAS), and X-ray absorption near edge structure (XANES).

For microbiological analysis, fresh tissue must also be sent in properly labeled sterile container(s). The pathologist should be informed in advance of fresh tissue submission in order to set up technical procedures for processing of the time-sensitive tissue sample.

Fixed Soft Tissue

For standard histological examination and submission of tissue to specialized laboratories for processing and evaluation, fixation in formalin is still the gold standard. The tissue should be placed in formalin (10% buffered formaldehyde) in a labeled and tightly sealed container. The ideal ratio of tissue volume to formalin volume is 1:3 to 1:10. For larger samples, a container of appropriate size should be used.

Fixed Bone Tissue

Bone tissue is also fixed in formalin. Decalcification is usually carried out with commercial solution using an acid decalcifying agent along with an added citrate buffer to help prevent cellular swelling and distortion during the process or with a mild solution such as ethylenediaminetetraacetic acid (EDTA). Both of them work well for immunohistochemical reactions.

For evaluation of metabolic bone conditions such as osteopenia, osteomalacia, and renal osteodystrophy, undecalcified bone sections in resin are required after fixation in Carnoy's solution (glacial acetic acid:chloroform:alcohol in a ratio of 1:3:6) and dehydration in ethanol before the resin embedding process.

Macroscopic Examination

Macroscopic examination is a very important part of the tissue processing that can significantly affect the histological diagnosis. Tissue description should be reported with accurate measurement of each sample and extensive sampling performed, optimally with no less than five tissue blocks/case. Pictures of the implant components should always be taken, and of tissue specimens when appropriate. Arthroscopy and ultrasound-guided needle biopsy specimens should be submitted in their entirety. In particular for needle core biopsy samples, the specimens should not be left in formalin solution for more than 2–3 h so as to avoid curling and twisting of the cores. Furthermore, they should be described at macroscopic examination with recording of the number and relative dimensions, collected with tweezers and arranged in parallel in the processing cassette between two foam pad inserts to preserve orientation, subject to standard processing, embedded parallel and slightly oblique, cut in four different tissue block levels at 5-μm thickness, and stained with standard H&E.

Take-Home-Message

- Pertinent clinical data and the type of prosthesis should be available to the pathologist at the time of histological examination.
- Each of the tissue samples (three to six tissue samples) measuring at least 1–3 cm should be collected at implant revision surgery "close to the prosthesis" and "far from the prosthesis," and osseous tissue should also be collected when feasible.
- Each of the tissue samples collected during arthroscopy (three to six samples) should have a diameter of at least 1 cm.
- The collection site of the tissue samples must be recorded for the analysis of the distribution of the wear material.
- Tissue samples should be extensively sampled at macroscopic examination with tissue sections taken according to the size of the specimen.
- The cellularity and type/amount of the wear particles should be routinely recorded semi-quantitatively (none, slight, moderate, marked) in the microscopic description of the pathology report.

5 Future Perspectives

5.1 Implant Wear Materials and Host Response

Every foreign material in the body initiates some kind of biological response. Studies that include systematic histological examinations with an adequate number of tissue samples (implant revisions and autopsy studies) could expand our understanding of the biological responses to the wear of implant materials. It would be desirable to also include in vitro studies that investigate the influence of wear particles from the various materials and their physicochemical features (chemical composition, size, shape, surface, quantity, resistance to corrosion) on the biological activity of the cells and their interactions. This method could give us a better understanding of the complex processes that occur at the biological/technical interface in vivo and that may lead to various modalities of implant failure [61] [62] [63].

5.2 Detection of Implant Infection at an Early Stage of Development

A promising field in the diagnosis and treatment of the complication of infection could be the development of new methods for detection of biofilms in vivo applied to arthroscopic examinations for detecting septic loosening at an early stage. However, currently, the successful treatment of orthopedic implant-related infections still relies on a traditional, combined surgical and antimicrobial therapy [64], [65].

5.3 Detection of Implant-Associated Adverse Reactions In Vivo at an Early Stage of Development

The projected dramatic increase in joint replacements in the next two decades makes the early detection of faulty implants on the market and the reduction of the occurrence of ALTR due to different cellular mechanisms leading to implant revision an important public health problem to be addressed with urgency. Although the lymphocytic reaction with tissue necrosis predominantly occurring in hip MoM implants has attracted the most attention in the past few years because of the short time of implantation before evidence of clinical symptoms and its rapid progression with a need for long-term follow-up to monitor the effects of chromium and cobalt toxicity [66], a more frequent reason for revision common to hip and knee joint prostheses, independent from the bearing surface, is loosening of the implant. Implant loosening is often associated with a considerable loss of bone and is divided into septic osteomyelitis secondary to infection and aseptic secondary to the invasion of wear particle-laden macrophages and increased osteoclastic activity and/or poor osseointegration of the implant components. Implant beds with this type of damage make revision surgery considerably more challenging because new implants can be more difficult to anchor. This type of adverse reaction is usually silent and of long duration before

clinical manifestations become evident. Therefore prevention or early detection of this potentially severe complication could help to identify susceptible patients or to stratify risk groups with a standardized surveillance protocol.

The ideal solution would be the development of a panel of cell markers to identify patients at risk in advance; however, this is not possible at present because of the limited knowledge of the factors driving the macrophagic response to different wear particles. Therefore, surveillance is mainly postoperative and relies on various radiological modalities such as computed tomography (CT) scan and multi-acquisition variable-resonance image combination (MAVRIC) magnetic resonance imaging (MRI). Moreover, these techniques also provide useful information regarding the location and extension of the osteolysis when it is already clinically suspected or evident. Radiostereometric analysis (RSA) can be used for early detection of incipient osteolysis. RSA is the most accurate technique for the measurement of implant component migration following total and/or resurfacing hip arthroplasty and can detect continuous migration long before clinical failure, making it a sensitive and reliable method for the evaluation of new implant designs and/or coatings [67], [68]. In The Netherlands and Scandinavia, RSA has therefore become mandatory before placing new artificial joints on the market. However, RSA provides accurate information about incipient loosening of an implant without identification of the underlying cause, and to date it has not been part of routine clinical use.

The development of new diagnostic tools using RSA would enable the differential clarification of the causes for at-risk implants. There are sensor techniques for use during arthroscopy that are currently being developed that will enable in vivo biofilm detection after preceding RSA. In particular, low-grade infections with SLIM types II and III could be identified and treated much earlier so that as much bone substance as possible could be preserved to ensure a good implant bed for revision [64]. The development of new algorithms or the integration of RSA into existing algorithms also appears useful for detecting other implant-associated pathologies.

5.4 Cellular Quantification and Threshold Determination for Adverse Reactions

Evaluation of the cell content in the neo-synovial membrane is used for a more accurate histological diagnosis and also to establish possible thresholds/patterns for specific pathological reactions, such as bacterial low-grade infections diagnosed via $CD15^+$ cell count [30]. Although ALTRs associated with corrosion products are characterized by the presence of a heterogeneous population of leukocytes with variable ratios [20], research is in progress to try to establish a $CD3^+$, T-cell threshold. The aim would be to differentiate nonspecific T-cell infiltrate, either interstitial and/or perivascular, from the one associated with particle-induced macrophagic infiltrate and/or hypersensitivity/allergy to metallic wear debris, either conventional and/or generated by corrosion. The task is particularly challenging because of the variable amount of infiltrate in different areas of the periprosthetic tissue, the possibility of mixed toxic/allergic reactions, and the variable quantitative

and qualitative response of the ALTR even within the same implant configuration. The association of a T-cell infiltrate with an increased number of mast cells and/or eosinophilic infiltrate, with or without the formation of germinal centers, could also provide an additional index for differentiating between allergic and nonallergic reactions [4].

6 Conclusion

Histological evaluation of the periprosthetic soft and osseous tissues is an important analytical tool to assess the physical and chemical composition of the implant wear particulate materials and the various types of host reactions to them and/or infection. Its standardization is essential to generate accurate and reproducible data that allow for comparisons in academic institutions, arthroplasty registries, and government regulatory agencies worldwide. It is also part of a multidisciplinary evaluation of orthopedic implant failures and provides valuable information to be integrated with the clinical data, allergological tests, radiological examinations, microbiological analyses, and biomechanical assessments of the implant wear.

Abbreviations

ALTR	Adverse local tissue reaction
ALVAL	Aseptic lymphocyte dominated vasculitis-associated lesion
ARMD	Adverse reaction to metallic debris
BSEM	Back-scatter scanning electron microscopy
CD	Cluster of differentiation (surface properties of leukocytes)
CoC	Ceramic-on-ceramic
CoCr	Cobalt-chromium
CoP	Ceramic-on-polyethylene
CT	Computerized tomography
DAPI	Diamidino-phenylindole
DMN	Dual modular neck
EDS	Energy dispersive X-ray spectroscopy
EDTA	Ethylenediaminetetraacetic acid
EM	Electron microscopy
FFPE	Formalin-fixed paraffin-embedded tissue
FISH	Fluorescent in situ hybridization
FTIR	Fourier transform infrared spectroscopy

H-E	Hematoxylin and eosin staining (standard histological staining method)
HPF	High-power field
HRA	Hip resurfacing arthroplasty
HXLPE	Highly cross-linked polyethylene
ICP-AES	Inductively coupled plasma atomic emission spectroscopy
IHC	Immunohistochemistry
MAS	Metallic adapter sleeve
MAVRIC	Multi-acquisition variable-resonance image combination
MoM	Metal-on-metal
MoP	Metal-on-polyethylene
MRI	Magnetic resonance imaging
PBR	Prussian blue reaction
PCR	Polymerase chain reaction
PE	Polyethylene
PMMA	Polymethyl methacrylate
PMN	Polymorphonuclear leukocyte
POL	Polarization optical analysis
RNA	Ribonucleic acid
RSA	Radiostereometric analysis
SEM	Scanning electron microscopy
SLIM	Synovial-like interface membrane
TEM	Transmission electron microscopy
THA	Total hip arthroplasty
UHMWPE	Ultra-high-molecular-weight polyethylene
XANES	X-ray absorption near edge structure
XAS	X-ray absorption spectroscopy
XRD	X-ray diffraction spectrometry

Acknowledgments

We would like to acknowledge Simone Giak for her expert secretarial and editorial assistance, Irina Shuleshko and Yana Bronfman for technical assistance in histology preparation, and Philip Rusli for formatting and editing of the illustrations.

References

[1] Kurtz S, Ong K, Lau E, et al (2007) Projections of primary and revision hip and knee arthroplasty in the United States from 2005 to 2030. J Bone Joint Surg Am 89-A:780-785
[2] Patel A, Pavlou G, Mujica-Mota, RE, et al (2015) The epidemiology of revision total knee and hip arthroplasty in England and Wales. Bone Joint J 97-B:1076-1081
[3] Krenn V, Morawietz L, Perino G, et al (2014) Revised histopathological consensus classification of joint implant related pathology. Pathol Res Pract 210(12):779-786
[4] Ricciardi B, Nocon AA, Jerabeck SA, et al (2016) Histopathological characterization of corrosion product associated adverse local tissue reaction in hip implants: a study of 285 cases. BMC Clin Pathol. doi:10.1186/s12907-016-0025-9
[5] Morawietz L, Classen RA, Schröder JH, et al (2006) Proposal for a histopathological consensus classification of the periprosthetic interface membrane. J Clin Pathol 59:591-597
[6] Krenn V, Thomas P, Thomsen M, et al (2014) Histopathological particle algorithm. Particle identification in the synovia and the SLIM. Z Rheumatol 73(7):639-649
[7] Schaumburger J, Lechler P, Grifka J, et al (2011) Histological pathological investigations and arthroplasty: do they make sense? Z Rheumatol 70(4):281-283
[8] Zmistowski B, Della Valle C, Bauer TW et al (2014) Diagnosis of periprosthetic joint infection. J Orthop Res 32:S98-S107
[9] Enayatollahi MA, Parvizi J (2015) Diagnosis of infected total hip arthroplasty. Hip Int 25(4):294-300
[10] Kriegsmann J, Hopf T, Jacobs D, et al (2009) Applications of molecular pathology in the diagnosis of joint infections. Orthopäde 38(6):531-538
[11] Gollwitzer H, Burgkart R, Diehl P, et al (2006) Therapy of arhtrofibrosis after total knee arthroplasty. Orthopäde 35:143-152
[12] Abdul N, Dixon D, Walker A, et al (2015) Fibrosis is a common outcome following total knee arthroplasty. Sci Rep 5:16469
[13] Faust I, Traut P, Nolting F, et al (2015) Human xylosyltraferases – mediators of arthrofibrosis? New patho-mechanistic insights into arthrofibrotic remodeling after knee replacement therapy. Sci Rep 5:12537
[14] Ruppert M, Theiss C, Knöß P, et al (2013) Histopathological, immunohistochemical criteria and confocal laser-scanning data of arthrofibrosis. Pathol Res Pract 209(11):681-688
[15] Thomas P, Braathen LR, Dörig M, et al (2009) Increased metal allergy in patients with failed metal-on-metal hip arthroplasty and periimplant T-lymphocytic inflammation. Allergy 64(8):1157-1165
[16] Granchi D, Cenni E, Giunti A, et al (2012) Metal hypersensitivity testing in patients undergoing joint replacement. J Bone Joint Surg Br 94-B:1126–1134
[17] Thyssen JP, Jakobsen SS, Engkilde K, et al (2009) The association between metal allergy, total hip arthroplasty, and revision. Acta Orthopaed 80(6):646-652
[18] Huber M, Reinis G, Trettenhahn G, et al (2009) Presence of corrosion products and hypersensitivity-associated reactions in periprosthetic tissue after aseptic loosening of total hip replacements with metal bearing surfaces. Acta Biomater 5(1):172-180
[19] Natu S, Sidaginamale RP, Gandhi J, et al (2012) Adverse reactions to metal debris: histopathological features of periprosthetic soft tissue reactions seen in association with failed metal on metal hip arthroplasties. J Clin Pathol 65(5):409–418
[20] Perino G, Ricciardi BF, Jerabek SA, et al (2014) Implant based differences in adverse local tissue reaction in failed total hip arthroplasties: a morphological and immunohistochemical study. BMC Clin Pathol 14:39. doi:10.1186/1472-6890-14-39
[21] Whitehouse MR, Endo M, Zachara S, et al (2015) Adverse local tissue reactions in metal-on-polyethylene total hip arthroplasty due to trunnion corrosion: the risk of misdiagnosis. Bone Joint J 97-B(8):1024-1030
[22] Mahendra G, Pandit H, Kliskey K, et al (2009) Necrotic and inflammatory changes in metal-on-metal resurfacing hip arthroplasties. Acta Orthop 80(6):653-659
[23] Mittal S, Revell M, Barone F, et al (2013) Lymphoid aggregates that resemble tertiary lymphoid organs define a specific pathological subset in metal-on-metal hip replacements. PLoS One 8(5):e63470
[24] Koulouvaris P, Ly K, Ivashkiv L, et al (2008) Expression profiling reveals alternative macrophage activation and impaired osteogenesis in periprosthetic osteolysis. J Orthop Res 26(1):106-116

[25] Cobelli N, Scharf B, Crisi GM, et al (2008) Mediators of the inflammatory response to joint replacement devices. Nat Rev Rheumatol 7:600-608
[26] Burton L, Paget D, Binder N, et al (2012). Orthopedic wear debris mediated inflammatory osteolysis is mediated in part by NALP3 inflammasone activation. *J Orthop Res*; 26:73-80.
[27] Huber M, Reinisch G, Zenz P, et al (2010) Postmortem study of femoral osteolysis associated with metal-on-metal articulation in total hip replacement. J Bone Joint Surg Am 92-A:1720-1731
[28] Fink B, Gebhard A, Fuerst M, et al (2013) High diagnostic value of synovial biopsy in periprosthetic joint infection of the hip. Clin Orthop Relat Res 471(3):956-964
[29] Morawietz L, Tiddens O, Mueller M et al (2009) Twenty-three neutrophil granulocytes in 10 high-power fields is the best histopathological threshold to differentiate between aseptic and septic endoprosthesis loosening. Histopathology 54(7):847–853
[30] Kölbel B, Wienert S, Dimitriadis J, et al (2015) CD15 focus score for diagnostics of periprosthetic joint infections: Neutrophilic granulocytes quantification mode and the development of morphometric software (CD15 quantifier). Z Rheumatol 74(7):622-630
[31] Thomas P, von der Helm C, Schopf C, et al (2015) Patients with intolerance reactions to total knee replacement: combined assessment of allergy diagnostics, periprosthetic histology, and peri-implant cytokine expression pattern. Biomed Res Int. doi:10.1155/2015/910156
[32] Mitchelson AJ, Wilson CJ, Mihalko WM, et al (2015) biomaterial hypersensitivity: is it real? supportive evidence and approach considerations for metal allergic patients following total knee arthroplasty. Biomed Res Int. doi:10.1155/2015/137287
[33] Thomas P, Schuh A, Ring J, et al (2008). Orthopedic surgical implants and allergies: joint statement by the implant allergy working group (AK 20) of the DGOOC (German association of orthopedics and orthopedic surgery), DKG (German contact dermatitis research group) and dgaki (German society for allergology and clinical immunology). Orthopäde 37(1):75-88
[34] Schäfer T, Böhler E, Ruhdorfer S, et al (2001) Epidemiology of contact allergy in adults. Allergy 56(12):1192-1196
[35] Thyssen JP, Menné T (2010) Metal allergy-A review on exposures, penetration, genetics, prevalence, and clinical implications. Chem Res Toxicol 23(2):309-318
[36] Bircher A, Friederich NF, Seelig W, et al (2012) Allergic complications from orthopaedic joint implants: the role of delayed hypersensitivity to benzoyl peroxide in bone cement. Contact Dermatitis 66(1):20-26
[37] Zustin J, Amling M, Krause M, et al (2009) Intraosseous lymphocytic infiltrates after hip resurfacing arthroplasty: a histopathological study on 181 retrieved femoral remnants. Virchows Arch 454(5):581-588
[38] Gilbert JL, Sivan S, Liu Y, et al (2015) Direct in vivo inflammatory cell-induced corrosion of CoCrMo alloy orthopedic implant surfaces. J Biomed Mater Res A 103(1):211-223
[39] Di Laura A, Hothi HS, Meswania JM, et al (2015) Clinical relevance of corrosion patterns attributed to inflammatory cell-induced corrosion: A retrieval study. J Biomed Mater Res B Appl Biomater. doi:10.1002/jbm.b.33540
[40] Reddy A, Caicedo MS, Samelko L, et al (2014) Implant debris particle size affects serum protein adsorption which may contribute to particle size-based bioreactivity differences. J Long Term Eff Med Implants 24(1):77-88
[41] Loeschner K, Harrington CF, Kearney JL, et al (2015) Feasibility of asymmetric flow field-flow fractionation coupled to ICP-MS for the characterization of wear metal particles and metalloproteins in biofluids from hip replacement patients. Anal Bioanal Chem 407(16):4541-4554
[42] Krenn V, Morawietz L, Kienapfel H, et al (2013) Revised consensus classification: histopathological classification of diseases associated with joint endoprostheses. Z Rheumatol 72(4):383-392
[43] Krenn V, Hopf F, Thomas P, et al (2016) Supramacroparticulate polyethylene in inflammation of synovial-like interface membranes: characterization and suggested nomenclature. Orthopäde 45(3):256-265
[44] Kubo T, Sawada K, Hirakawa K, et al (1999) Histiocyte reaction in rabbit femurs to UHMWPE, metal, and ceramic particles of different sizes. J Biomed Mater Res 45(4):363-369
[45] Otto M, Kriegsmann J, Gehrke T, et al (2006) Wear particles: key to aseptic prosthetic loosening? Pathologe 27(6):447-460
[46] Mirra JM, Amstutz HC, Matos M, et al (1976) The pathology of the joint tissues and its clinical relevance in prosthesis failure. Clin Orthop Relat Res 117:221-240
[47] Doorn PF, Mirra JM, Campbell PA, et al (1996) Tissue reaction to metal-on-metal total hip prosthesis. Clin Orthop Relat Res 329:S221-S40
[48] Xia Z, Kwon YM, Mehmood S, et al (2001) Characterization of metal-wear nanoparticles in pseudotumor following metal-on-metal hip resurfacing. Nanomedicine 7(6):674–681

[49] Xia Z, Ricciardi BF, Zhao Liu, et al (2016) Nano-analyses of Wear Particles from Metal-on-Metal and Non-Metal-on-Metal Dual Modular Neck Hip Arthroplasty. Nanomedicine: doi.org/10.1016/j.nano.2016.11.003
[50] Brach del Prever EM, Bistolfi A, Bracco P, et al (2009) UHMWPE for arthroplasty: past or future? J Orthopaed Traumatol 10:1-8
[51] Catelas I, Wimmer MA (2011) New insights into wear and biological effects of -on-metal bearings. J Bone Joint Surg Am 93 Suppl 2:S76-S83
[52] Hart AJ, Quinn PD, Sampson B, et al (2010) The chemical form of metallic debris in tissues surrounding metal-on-metal hips with unexplained failure. Acta Biomater 6(11):4439-4446
[53] Willert HG, Buchhorn GH, Fayyazi A, et al (2005) Metal-on-metal bearings and hypersensitivity in patients with artificial hip joints. A clinical and histomorphological study. J Bone Joint Surg Am 87A:28–36
[54] Bal SB, Garino J, Ries M, et al (2006) Ceramic materials in total joint arthroplasty. Semin Arthro 17:94-101
[55] Macdonald N, Bankes M (2014) Ceramic on ceramic hip prostheses: a review of past and modern materials. Arch Orthop Trauma Surg 134:1325-1333
[56] Savarino L, Baldini N, Ciapetti, G, et al (2009) Is wear debris responsible for failure in alumina-on-alumina implants? Clinical, histological, and laboratory investigations of 30 revision cases with a median follow-up time of 8 years. Acta Orthop 80(2):162-167
[57] Krenn V, Thomas P, Thomsen M (2015) Histopathological differential diagnosis of implant intolerance. Working Group 11 of the DGOOC: Implant Intolerance. ISBN 978-3-00-050115-9
[58] Hayter CL, Gold SL, Koff MF, et al (2012) Findings in painful metal-on-metal hip arthroplasty. AJR Am J Roentgenol 199:884–893
[59] Nawabi DH, Hayter CL, Su EP, et al (2013) Magnetic resonance imaging findings in symptomatic versus asymptomatic subjects following metal-on-metal hip resurfacing arthroplasty. J Bone Joint Surg Am 95A:895–902
[60] Hügle T, Leumann A, Pagenstert G, et al (2014) Retrograde synovial biopsy of the knee joint using a novel biopsy forceps. Arthrosc Tech 53(3):317-319
[61] Pourzal R, Cichon R, Mathew MT, et al (2014) Design of a tribocorrosion bioreactor for the analysis of immune cell response to *in situ* generated wear products. J Long Term Eff Med Implants 24(1):65-76
[62] Scharf B, Clement CC, Zolla V, et al (2014) Molecular analysis of chromium and cobalt-related toxicity. Sci Rep 4:5729
[63] Rakow A, Schoon J, Dienelt A, et al (2016) Influence of particulate and dissociated metal-on-metal hip endoprosthesis wear on mesenchymal stromal cells *in vivo* and *in vitro*. Biomater 98:31-40
[64] Sesselmann S, Hausotte T, Timmermann M et al (2015) Radiostereometric analysis as a need for early detection of septic loosening. EC Orthopaedics 2(3):89-96
[65] Sendi P and Zimmerli W (2012) Antimicrobial treatment concepts for orthopedic device-related infection. Clin Microbiol Infect 18:1176-1184
[66] Keegan GM, Learmonth ID, Case CP (2008) A systematic comparison of the actual, potential, and theoretical health effects of cobalt and chromium exposures from industry and surgical implants. Crit Rev Toxicol 38:645-674
[67] Böttner F, Su E, Nestor B, et al (2005) Radiostereometric analysis: the hip. HSSJ 1:94-99
[68] Sesselmann S, Forst R, Tschunko F (2013) Radiostereometric analysis of hip implants – a critical review of methodology and future directions. OA Musculoskeletal Medicine 1(4):31

Clinical Management of Joint Arthroplasty

The volumes of the Clinical Management Guide series are directed at orthopaedic surgeons who want to acquire information rapidly while saving as much time as possible. As a helpful advisory tool, this Pocket Guide concisely and clearly imparts the current state of knowledge on selected issues of everyday clinical practice and, in doing so, concentrates purely on the essential.

In addition, it also addresses medical practitioners and scientists of adjacent specialist disciplines who are not confronted on a daily basis with problems regarding endoprosthetics but, when required, would like to access important information on a specific topic.

Periprosthetic Tissue Pathologies

This guide to the histological diagnosis of the periprosthetic tissue pathologies in joint arthroplasty is intended to provide a concise, yet comprehensive introduction to the host soft tissue and bone reactions to the implants and their wear particulate materials and a practical aid for tissue sampling and processing for optimal pathological analysis. The target audience is the orthopedic surgeons, either in practice or in training, and also the clinicians, radiologists, pathologists, and biomechanical engineers who are interested in understanding the details of the histological examination and report.

ISBN 978-3-662-54203-3

▶ springer.com